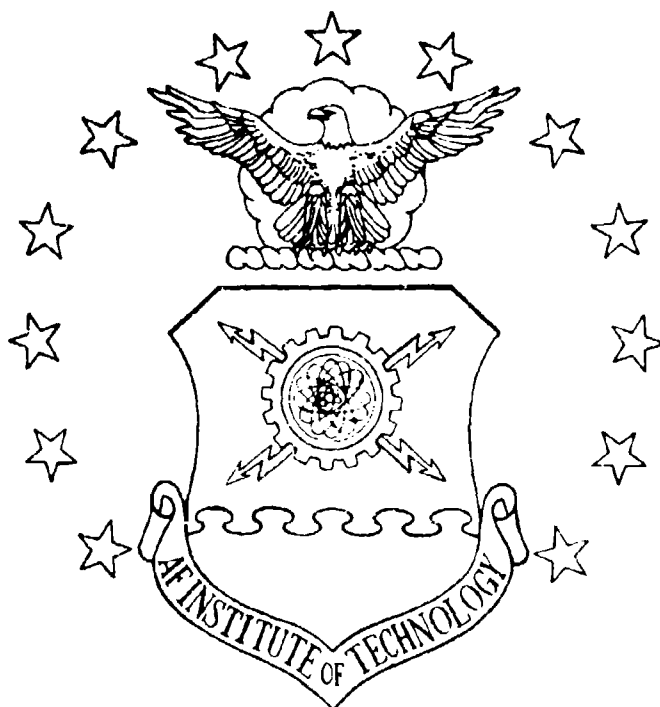


AD-A153 087

DTIC FILE COPY



CHARACTERISTICS OF A CONFINED JET  
THRUST VECTOR CONTROL NOZZLE

THESIS

Anthony J. Porzio  
Second Lieutenant, USAF

AFIT/GAE/AA/84D-22

**DISTRIBUTION STATEMENT A**

Approved for public release  
Distribution Unlimited

DEPARTMENT OF THE AIR FORCE  
AIR UNIVERSITY

**AIR FORCE INSTITUTE OF TECHNOLOGY**

Wright-Patterson Air Force Base, Ohio

DTIC  
ELECTE  
APR 30 1985  
B

AFIT/GAE/AA/84D-22

CHARACTERISTICS OF A CONFINED JET  
THRUST VECTOR CONTROL NOZZLE

THESIS

Anthony J. Porzio  
Second Lieutenant, USAF

AFIT/GAE/AA/84D-22

Approved for public release; distribution unlimited

DTIC  
ELECTE  
APR 30 1985  
S B D

AFIT/GAE/AA/84D-22

CHARACTERISTICS OF A CONFINED JET  
THRUST VECTOR CONTROL NOZZLE

THESIS

Presented to the Faculty of the School of Engineering  
of the Air Force Institute of Technology

Air University

In Partial Fulfillment of the  
Requirements for the Degree of  
Master of Science in Aeronautical Engineering

Anthony J. Porzio, B.E.  
Second Lieutenant, USAF

December 1984

Approved for public release; distribution unlimited

## Preface

The purpose of this report was to examine the characteristics of a confined jet thrust vector control (CJTVC) nozzle. Unlike some other thrust vector control devices using secondary injection, the CJTVC nozzle can operate at high altitudes by isolating an area of flow separation within the nozzle. Therefore, this type of nozzle may be useful in small missiles or spacecraft attitude control by eliminating hydraulic gimbaling systems or banks of several small directional thrusters.

Thanks to Dr. Milon Franke, my thesis advisor, I was able to take a thesis topic pretty much 'out of the blue' and do what I could with it. This meant building a two degree-of-freedom test stand that could monitor axial thrust and side force along with numerous pressure readings. Also, the control of a dozen secondary injection ports had to be accomplished. All this was accomplished using some existing equipment, a data acquisition and control system, and the ingenuity of the AFIT Shop. There are limitations in the system. Total pressure measurements in the nozzle cannot be made and there are no direct mass flow measurements. Flow visualization was done using oil streaking and a Schlieren optical system. Although both methods were useful, neither yielded images good enough to document. An attempt to use a plexiglass nozzle to enhance internal flow visualization ended in

catostrophic failure.

I'd like to thank Dr. Franke for his assistance in this effort along with giving me a pretty free hand in designing the experiment and deciding the scope of the project. My thanks also go to Dr. W.C. Elrod and Captain W.R. Cox for their assistance throughout the entire work. Finally, my thanks to the AFIT technicians, Nick Yardich, Leroy Cannon, and Harley Linville for their great support, and to John Brohas and Carl Shortt at the AFIT Shop for their exemplary work in fabricating the apparatus.

Anthony J. Porzio

Approved	✓
PER CALL JC	
A-1	



## Table of Contents

	Page
Preface .....	ii
List of Figures .....	vi
Notation .....	viii
Abstract .....	ix
I. Introduction .....	1
Background .....	1
Confined Jet Thrust Vector Control .....	2
Development of CJTVC .....	4
Objectives .....	4
II. Experimental Apparatus .....	7
Nozzle .....	7
Test Stand .....	7
Data Acquisition .....	12
Control .....	12
III. Experimental Procedure .....	14
IV. Results and Discussion .....	16
Axial Thrust .....	16
Efficiency .....	16
SI Pressure Effects .....	21
Side Force .....	23
SI Pressure Effects .....	23
SI Port Area Effects .....	26
Thrust Vector Angle .....	28
Flow Gain .....	28
Nozzle Instabilities .....	32
Undeflected Jet Instability .....	32
Vectoring Instability at Low SI Pressure .....	40
Undeflected Jet Instability with Four SI Ports Operating .....	42

V.	Conclusions .....	46
VI.	Recommendations .....	47
Appendix A:	Primary System and SI System Mass Flow Calculations .....	48
Appendix B:	Notes on CJTVC Numerical Analysis .....	51
Bibliography	.....	56
Vita	.....	57

## List of Figures

Figure	Page
1. Boundary Layer Thrust Vector Control .....	3
2. Confined Jet Thrust Vector Control .....	3
3. CJTVC Schematic .....	5
4. 24:1 CJTVC Nozzle .....	8
5. SI Section .....	8
6. Exit Orifice Section .....	9
7. SI Port Inserts .....	9
8. Schematic of the CJTVC Test Stand .....	10
9. SI Supply Manifold on Settling Tank .....	11
10. Axial Thrust vs. Primary Pressure .....	17
11. Undeflected Jet Pressure Distribution .....	18
12. Undeflected Jet Operation .....	20
13. Orifice Section Pitting .....	21
14. Axial Thrust vs. SI Pressure .....	22
15. Vectored Configuration Pressure Distribution ....	24
16. Side Force vs. SI Pressure .....	26
17. Side Force vs. SI Port Area .....	27
18. Thrust Vector Angle vs. SI Pressure .....	29
19. Side Force vs. Mass Flow Gain (Constant $A_j$ ) .....	30
20. Side Force vs. Mass Flow Gain .....	31
21. Upstream Transducers Strip Chart Traces During an Axial Instability .....	34
22. Downstream Transducer Strip Chart Trace During a Stable Vectoring .....	35
23. Downstream Transducer Strip Chart Trace During	



	an Axial Instability .....	36
24.	Axial Instability Scenario .....	38
25.	Downstream Transducer Strip Chart Trace During an Unstable Vectoring .....	41
26.	Test Output for Side Force vs. Time for Single- Port and Four-Port Operation .....	44
27.	SI System Flow Model .....	49
28.	Vectored Nozzle Network Model .....	52
29.	Axially Operating Nozzle Network Model .....	55

### Notation

$A_{eo}$  - Exit Orifice Area  
 $A_m$  - Maximum Nozzle Area  
 $A_i$  - Secondary Injection Port Area  
 $A_t$  - Throat Area  
 $P_o$  - Primary Supply Pressure  
 $P_i$  - Secondary Injection Supply Pressure  
 $PR$  - Supply Pressure Ratio

AFIT - Air Force Institute of Technology  
BLTVC - Boundary Layer Thrust Vector Control  
CJTVC - Confined Jet Thrust Vector Control  
SI - Secondary Injection

Abstract

A study of confined jet thrust vector control (CJTVC) is presented. By isolating an area of flow separation within the body of a nozzle, CJTVC has the advantage over other thrust vector control systems using secondary injection (SI) in that it can operate independent of altitude. This makes it ideal for applications in small missiles and spacecraft attitude control. In this study, axial thrust, side force, and pressure distribution across the nozzle were measured. The parameters varied were SI pressure, primary supply pressure, and SI port area.

Results indicate that there is a lower limit to the supply pressure ratio (SI pressure to primary pressure) and SI mass flow, below which, the nozzle will not produce side force. Also, above a primary pressure of 200 psig, the undeflected jet exhibits instabilities. Without SI, a 4 Hz oscillation occurs in the nozzle and switching jet attachment occurs near the throat. When an attempt is made to vector the nozzle at a below minimum SI pressure, a similar, but faster, 9 Hz oscillation begins. The production of side force is limited by choking of the SI ports. Mass flow gain, the ratio of primary mass flow to SI mass flow, and side force are both found to be functions of SI port area and supply pressure ratio.

# CHARACTERISTICS OF A CONFINED JET THRUST VECTOR CONTROL NOZZLE

## I. Introduction

### Background

Thrust vector control has always been a major area of research in the field of propulsion. The direction of a rocket's thrust is critical in controlling a vehicle's flight-path and attitude. Goddard's rockets were vectored using aerodynamic surfaces. von Braun's V2 missile used vanes in the rocket engine's exhaust plume. Today, the space shuttle's main engines and solid rocket boosters are vectored by gimbaling the engines and nozzles. Most spacecraft~~s~~ and strategic and tactical missiles built over the past 25 years have had thrust vector control systems using hydraulics to gimbal the physical engine or the rocket nozzle. Although this system has been proven time and again, it is not exempt from the constant struggle to lighten the weight of aerospace vehicles.

Eliminating heavy hydraulic machinery is an attractive goal in propulsion design. One promising and proven way of doing this in low altitude systems has been the use of boundary layer thrust vector control (BLTVC). This system uses secondary injection (SI) in an overexpanded rocket nozzle to create an area of separation that causes the thrust to leave the nozzle off-axis, creating a side force (1:2).

Figure 1 shows this system that has already been tested full scale (2). There is, however, one major drawback using BLTVC. The SI is achieved by opening ports downstream of the throat to ambient conditions. This is fine for operating at low altitude; however, for a BLTVC nozzle operating at high altitude, the nozzle flow expands to the point where opening an injection port has no effect on vectoring. What is needed here is a system using SI that can operate independent of altitude.

#### Confined Jet Thrust Vector Control

Confined jet thrust vector control (CJTVC) also utilizes the overexpanded nozzle and SI ports. However, downstream of the overexpanded nozzle, a cylindrical section and reconverging section are added. In this system, when SI ports are open, the area of separation that is created by the high pressure injection flow is contained within the body of the nozzle as shown in Figure 2. Also, by having the flow exit the nozzle at supersonic speeds, the area of separation operates independently of ambient conditions. This isolation makes the CJTVC nozzle ideal for space and high altitude applications.

The one obvious drawback of the system is the need for a secondary supply for the injectant flow. Although this adds weight and complexity to the system, the high gain of primary flow to secondary flow allows the use of small amounts of cold gas for injection. This pressurized gas can be stored in a small volume. Also, since a pressurized gas is

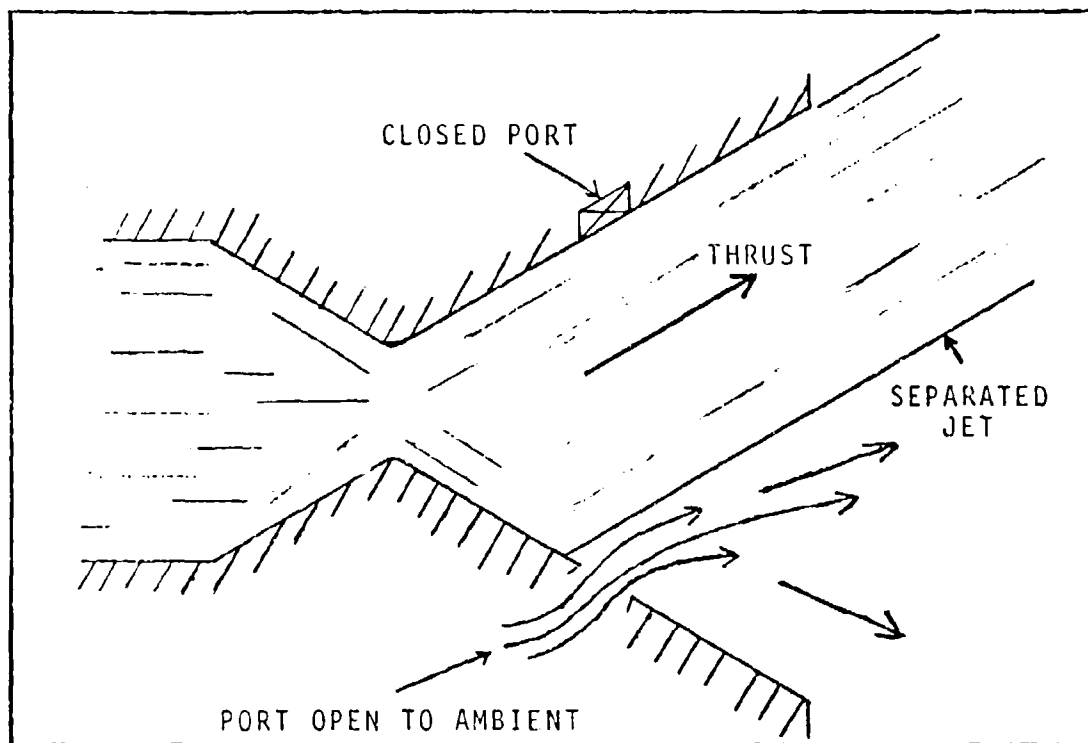


Figure 1. Boundary Layer Thrust Vector Control

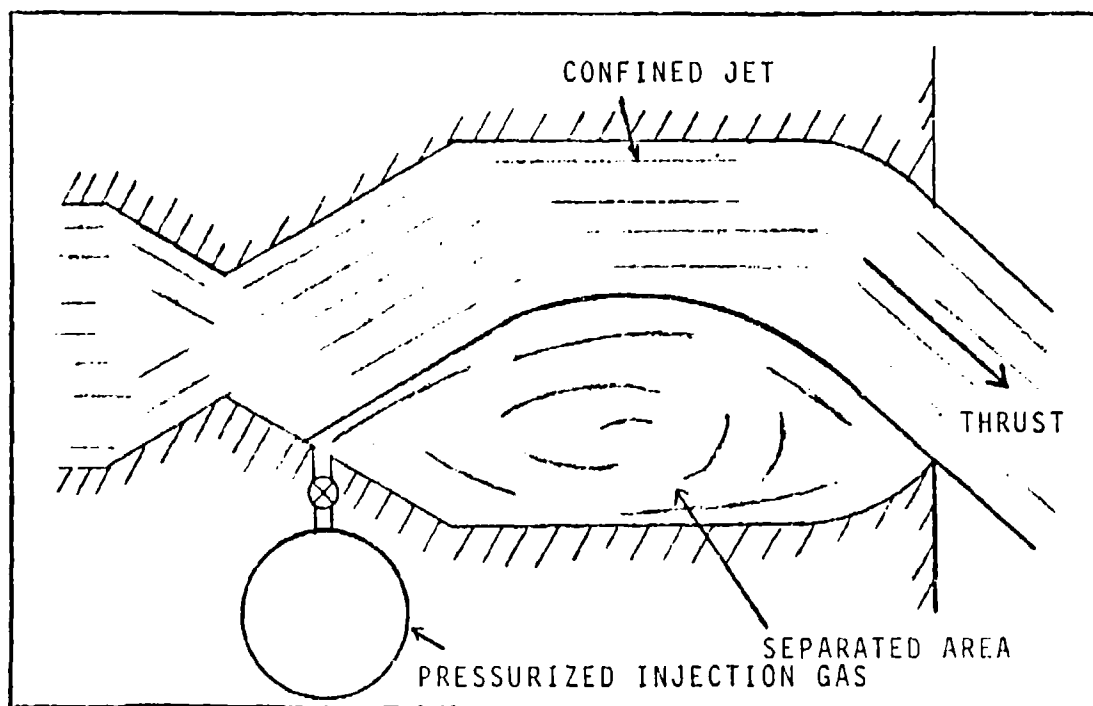


Figure 2. Confined Jet Thrust Vector Control

used, small and fast control valves can be incorporated into the SI supply system (3:10).

#### Development of CJTVC

CJTVC was studied extensively at Chandler Evans Control Systems where the basic operation was proven in a two dimensional form in 1971 (3:5). In 1975, development continued by proving vectoring capability in two planes along with the first hot flow tests. In 1976, further development continued under Navy funding. This included cold flow testing of numerous nozzle geometries and continued hot flow tests on some specific configurations.

By measuring the geometric effects on side force and axial thrust, Fitzgerald and Katz summarized their results into design data that were published in 1980 (3,4). These reports concluded that a nozzle with a thrust efficiency of 92% (the ratio of actual thrust to the thrust of an ideally expanded nozzle operating at the same supply to ambient pressure ratio) and a maximum vectoring angle of more than 25 degrees could be achieved with a 17:1 maximum area to throat area ratio. The optimum location of the SI ports was also defined. Figure 3 shows a schematic of a CJTVC nozzle that highlights the major geometric parameters.

#### Objectives

This study concentrated on continuing to define operational characteristics of CJTVC. To expand the number of

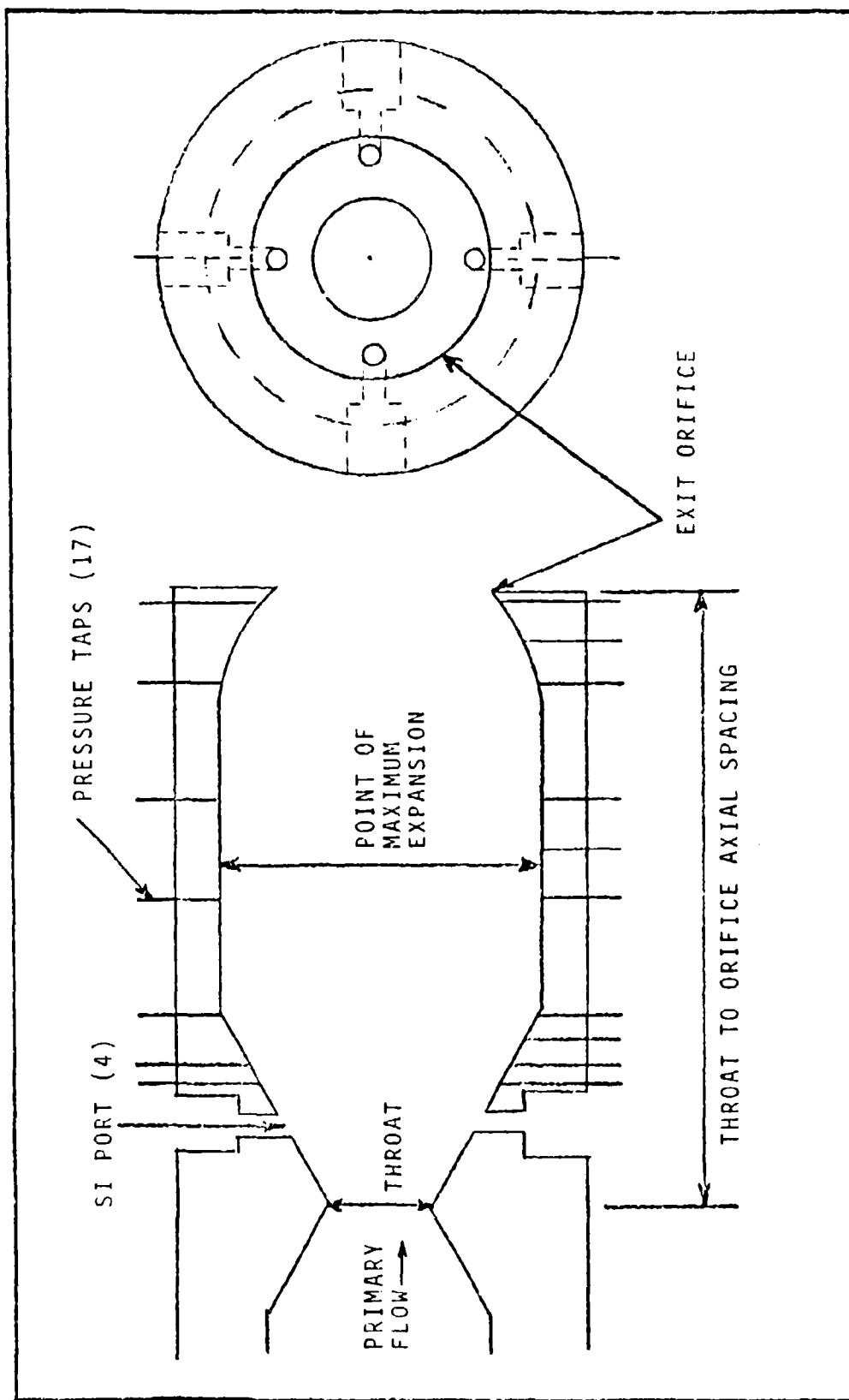


Figure 3. CJIVC Schematic



different configurations studied, a nozzle with a geometry different from those used at Chandler Evans was built and the following objectives were undertaken:

- 1) Verify general characteristics found by Fitzgerald and Katz
- 2) Examine the side force produced
- 3) Examine the axial thrust produced
- 4) Calculate the amount of SI mass flow needed to produce side force
- 5) Examine axial thrust stability
- 6) Examine vectoring stability.

## II. Experimental Apparatus

### Nozzle

The nozzle, Figure 4, was fabricated in three sections: 1) the mating section, 2) the SI section, and 3) the exit orifice section. The mating section holds the nozzle to the test stand and contains part of the converging contour. The SI section, Figure 5, contains the throat, SI ports, diverging contour, and cylindrical contour. The exit orifice section, Figure 6, contains the reconverging contour and the exit orifice. The three sections are held together by bolted flanges. There are seventeen static pressure taps in the nozzle. The SI section has twelve pressure taps and the orifice section, five. These are arranged in sets of three and two, 180 degrees apart. Each set is placed in each contour section. Two individual taps are located near two of the four SI ports. The SI ports are 3/16" in diameter and are capped with 1/4" hose connectors that are screwed into the wall of the nozzle. These connectors can be removed so that inserts can be put into the injection ports to change their diameters (Figure 7).

### Test Stand

Figure 8 shows a schematic of the test stand, flow system, and instrumentation. The nozzle is mounted on a tank that serves as a settling chamber. This tank is attached to a thrust measurement device that is basically a two degree-

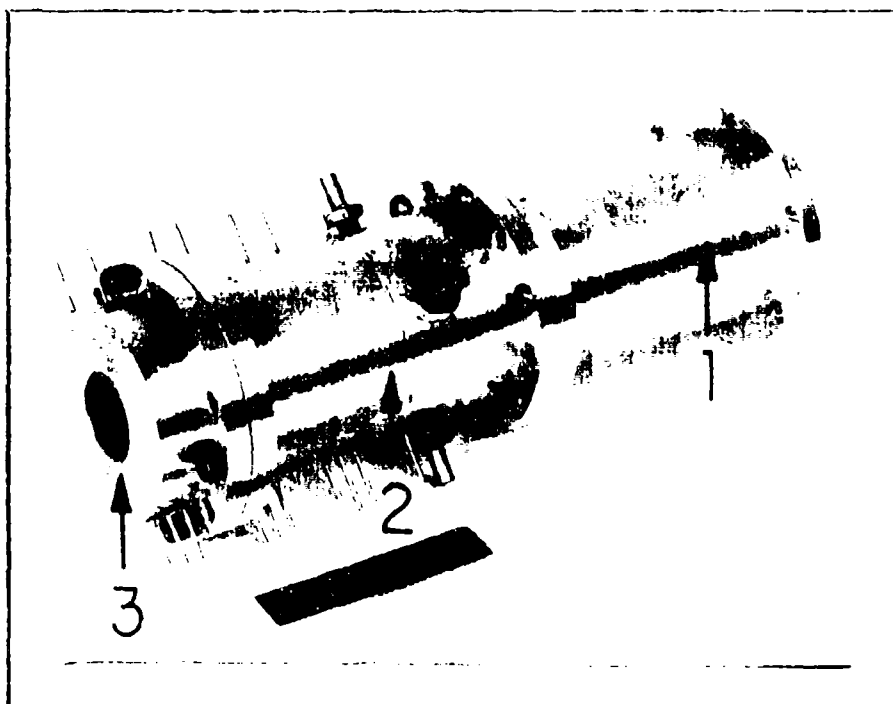


Figure 4. 24:1 CJTVC Nozzle

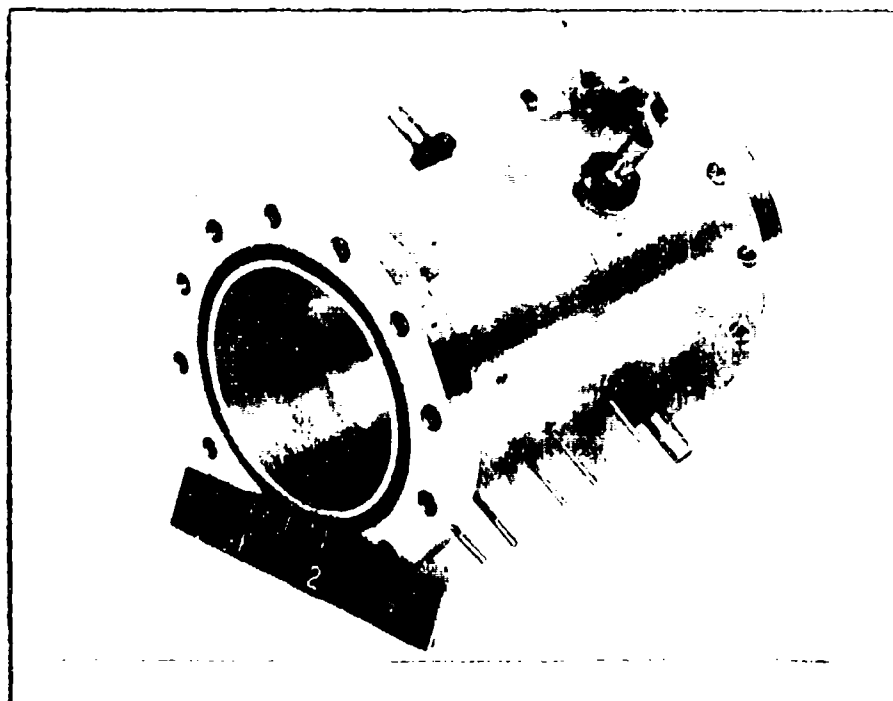


Figure 5. SI Section



Figure 6. Exit Orifice Section

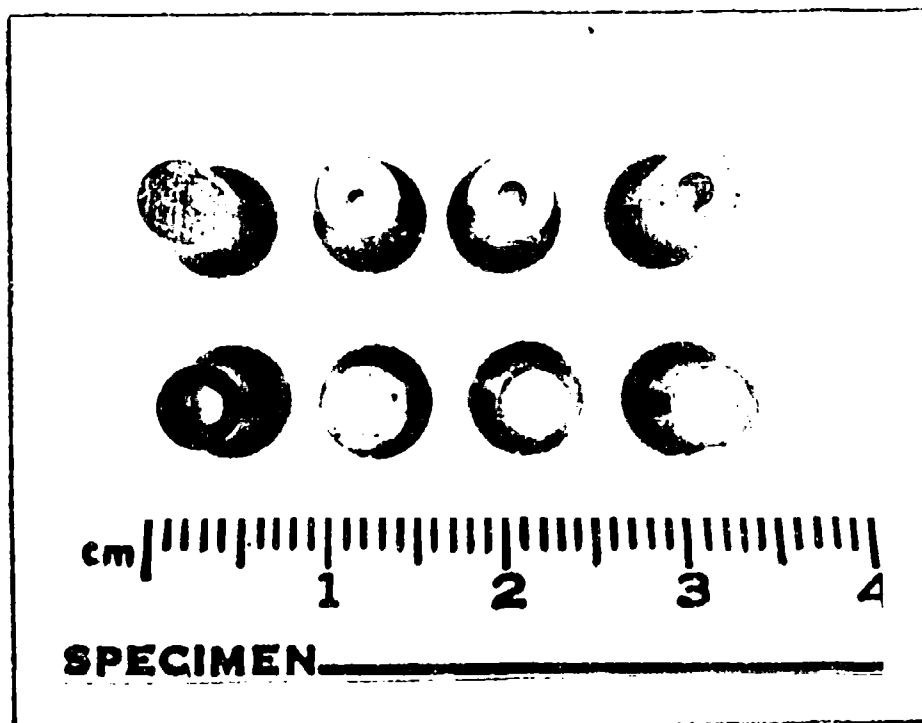


Figure 7. SI Port Inserts

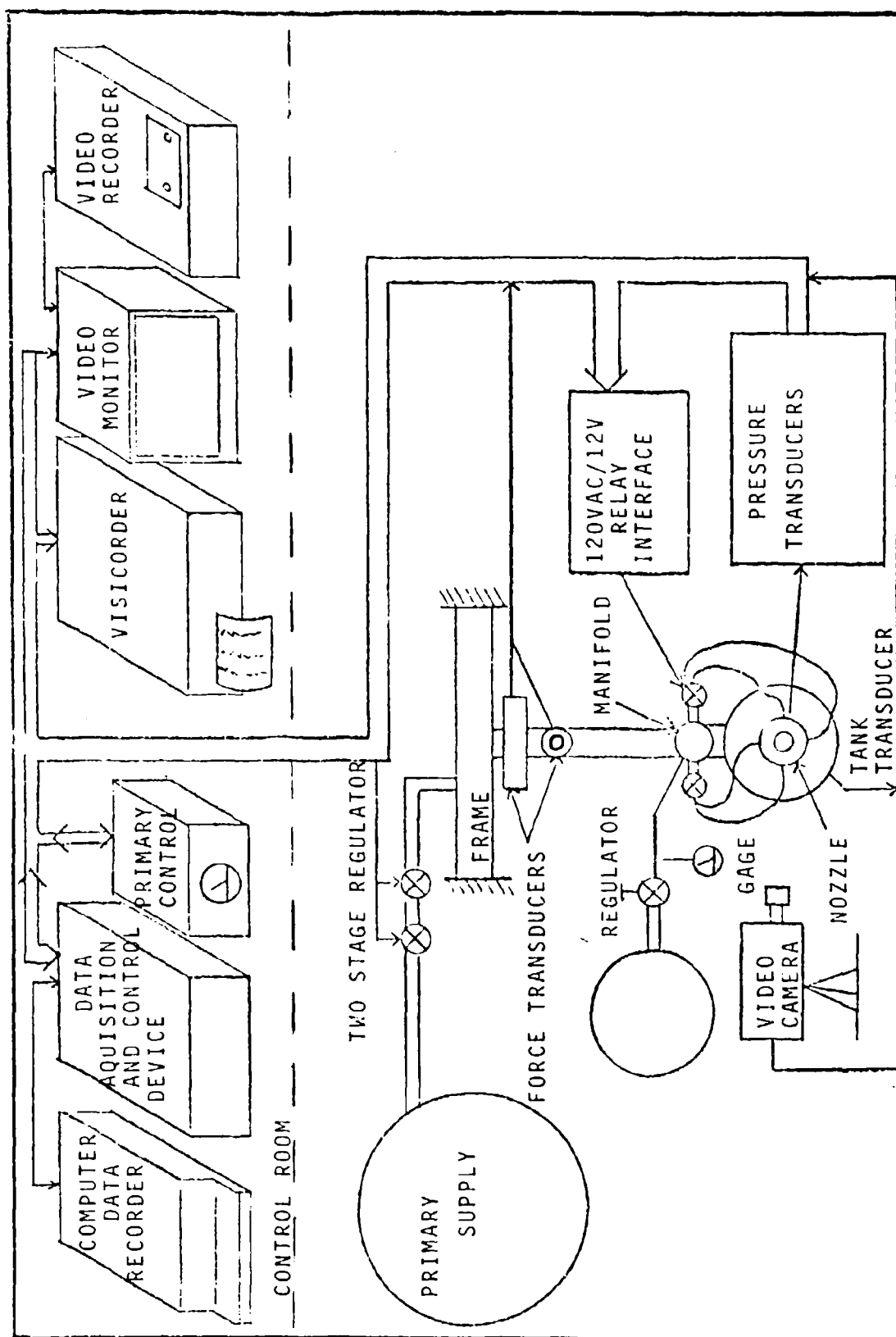


Figure 8. Schematic of the CJTVC Test Stand



Figure 9. SI Supply Manifold on Settling Tank

of-freedom pendulum. Side force and axial thrust are measured by force transducers mounted at the two pivot points. The entire system is hung from an 'A' frame and is anchored at several points.

The SI flow is supplied from a manifold that 'rides' on the tank in a saddle-like brace (Figure 9). The manifold is connected to its supply through a flexible hose which allows the tank to pivot freely. Secondary flow is taken from the manifold through solenoid valves which feed the SI ports through 1/4" flexible tubes. The pressure transducers are on a stand near the nozzle and are connected to the wall taps through 1/16" flexible tubes.

The pressure transducers are Statham bellows-type gages.

The force transducers were custom built for the test stand. They consisted of phenolic-backed foil strain gages mounted on 1/2" thick steel bars.

#### Data Acquisition

Pressure, side force, and axial thrust measurements were obtained and recorded on tape by a computer or recorded on strip charts through a galvanometer-type oscillograph. The computer system was capable of handling two force measurements and 17 pressure measurements from separate transducers or two force measurements and 48 pressure taps using a scanivalve in conjunction with a single transducer. The oscillograph could take continuous data from any three transducers. A Schlieren optical system was used for flow visualization. Both photographic and video information were recorded. Oil streaking was also used for flow visualization on the walls of the nozzle.

#### Control

The computer was used for control of the solenoid valves in the SI system. The computer was programmed to create a data file, open the desired SI valves, and record pressure and thrust measurements in the data file. The configuration of the valves could be changed at any time during a test. They could be opened or closed individually, pulsed in sets, or sequenced going clockwise or counterclockwise around the nozzle. The scanivalve, if it was used, could be commanded to step to the next port or 'home' back to port #0 at any

time during the test.

Control of the SI and primary supply pressure was accomplished without the computer. The primary supply was set from the control room through solenoid valves which loaded and vented dome valves in a two-stage regulator. This supply also had a remote controlled gate valve that could isolate the test stand from the supply. The SI system was controlled manually through a regulator/dome valve set and was adjusted before each test run.



### III. Experimental Procedure

The procedure for a typical test run was as follows:

- 1) The nozzle was configured for a specific test
- 2) The SI system pressure was set through the regulator/dome valve
- 3) The test area was cleared
- 4) The solenoid valve commands were stored in a data file
- 5) The master control program was loaded into the computer. This enabled the computer to read the solenoid valve commands and to create a test data file based on the test time duration
- 6) Ambient conditions, temperature and pressure, were recorded
- 7) On command from the computer, the primary supply system was activated
- 8) When the primary supply system reached the desired pressure, the computer was commanded to start the test
- 9) The computer ran the test, switching solenoid valves, and recording transducer output
- 10) On command from the computer at the end of a test, the primary supply dome valves were vented
- 11) The SI system was shut off and data were recorded on tape

After a test run, thrust and pressure measurements could be viewed directly using a data viewing program. This program

could read the transducer levels, solenoid valve configuration, and scanivalve configuration, and used recorded transducer characteristics to find the actual thrust and pressure.

Before each test run, a calibration program was run to record the zero output of the transducers. This information was also used by the data viewing program to increase the accuracy of the data by comparing these values to the calibrated zero outputs of the transducers.

#### IV. Results and Discussion

The characteristics of a CJTVC nozzle were studied by measuring the effects of primary pressure ( $P_o$ ), SI pressure ( $P_i$ ), and SI port area ( $A_i$ ) on axial thrust, side force, thrust vector angle, and mass flow gain. The efficiency of the CJTVC nozzle was measured and compared to the efficiency of conventional converging-diverging nozzles. Also, the instabilities exhibited by the nozzle during vectoring and undeflected states were studied.

##### Axial Thrust

Efficiency. The efficiency of a CJTVC nozzle is defined as the ratio of actual thrust to the thrust of an ideally expanded nozzle operating at the same supply to ambient pressure ratio. According to Fitzgerald and Kampe (3), a CJTVC nozzle with a 6:1 orifice expansion ratio ( $A_{eo}/A_t$ ) should be 89% efficient at all primary supply pressures and regardless of SI pressure. The measured efficiency of the nozzle tested was much lower. Over the primary pressure range of 100 to 500 psig, the mean efficiency was 57.9%. Although this seems to be a great deviation in the expected efficiency, there is actually no real change from the tests conducted by Fitzgerald and Katz. According to their data (3:15), for a nozzle with a 6:1 orifice expansion ratio, the throat to orifice spacing should be 8.5 throat diameters for optimum efficiency. The nozzle used incorporated a throat

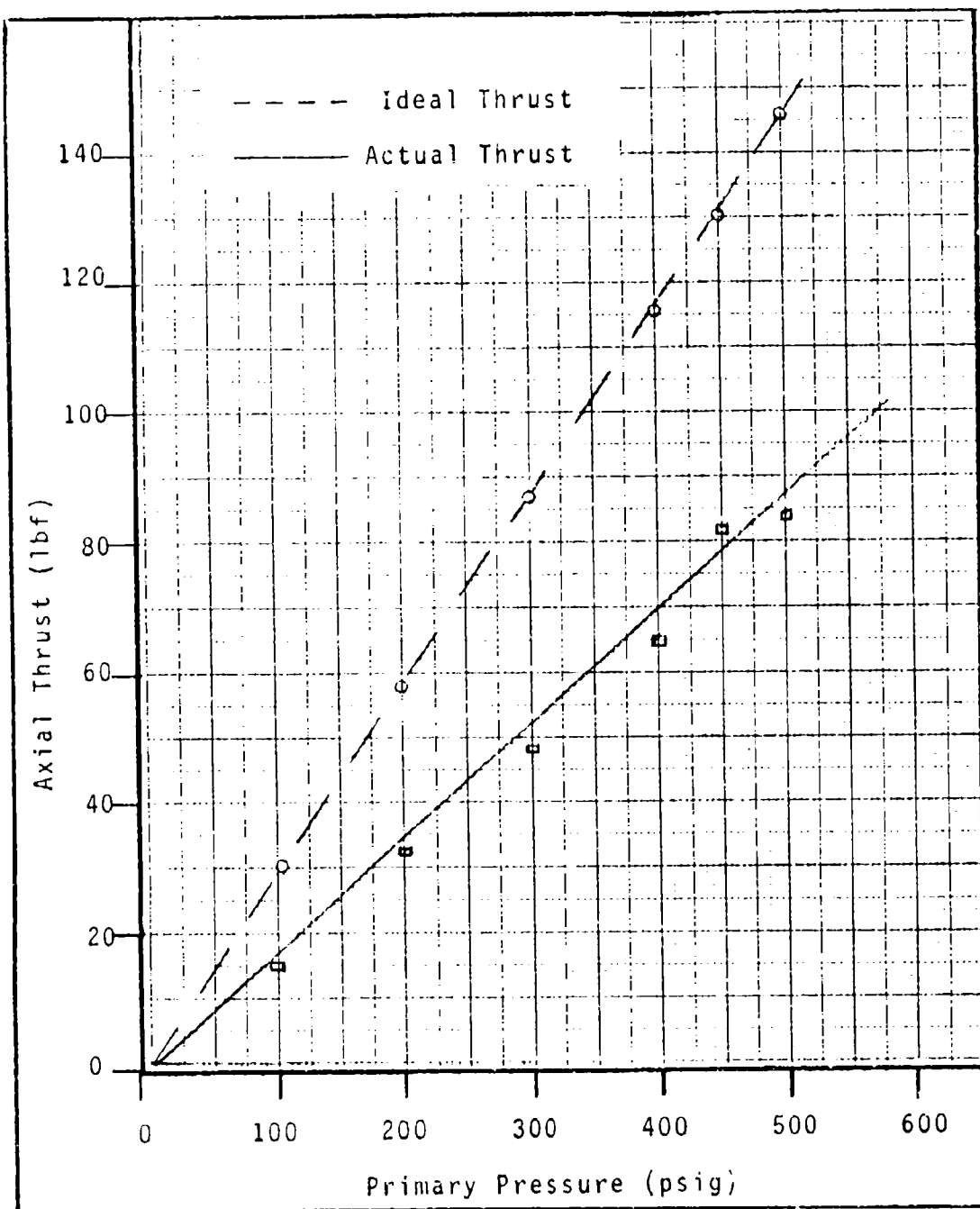


Figure 10. Axial Thrust vs. Primary Pressure

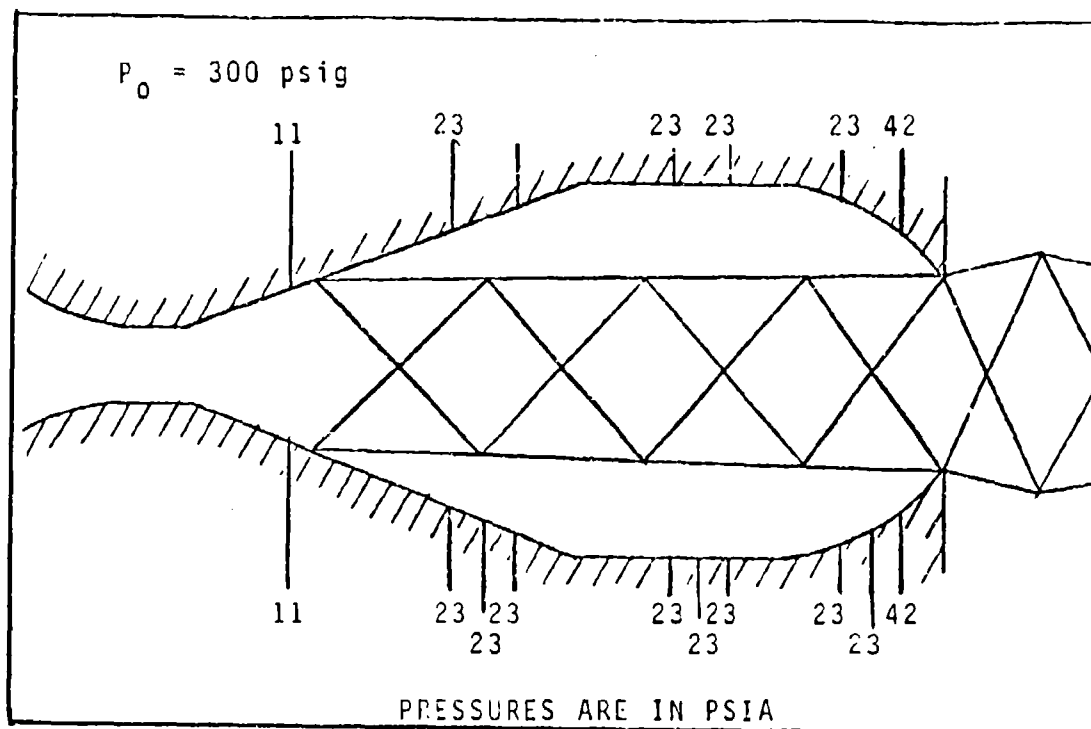


Figure 11. Undeflected Jet Pressure Distribution

to orifice spacing of 10.375 throat diameters. Fitzgerald and Katz stated (3:17) that a longer than optimum nozzle would yield a higher mass flow gain (the ratio of primary mass flow to SI mass flow), but lower efficiency. Figure 10 shows the actual thrust produced by the nozzle as a function of primary pressure.

Figure 11 shows a typical pressure distribution for the nozzle operating at a primary pressure of 300 psig. At the first set of pressure taps, low pressure indicated expansion of the flow past the SI ports. However, through the rest of the diverging section and the cylindrical section, the static pressure was higher and constant up to the orifice lip. This constant pressure most probably indicated

that there was a detached jet inside the nozzle since a subsonic flow or expanding supersonic flow would show some non-constant pressure distribution (5:73-159). The higher pressure at the lip of the exit orifice was due to the impinging jet since these taps had an appreciable projected area parallel to the nozzle axis, no longer yielding static pressure measurements.

Considering the pressure distribution of the undeflected jet, there is an hypothesis to explain the drop in efficiency for a nozzle that has a longer than optimum throat to orifice spacing. Figure 12 shows the jet detaching at a point where the area is somewhat less than that of the orifice as determined by Fitzgerald and Katz (3:17). They also determined that the jet spreaded at a half angle of 0.8 degrees until it leaves the nozzle through the orifice. As the jet leaves the nozzle, some of the flow impinges on the lip and is fed back into the separated area, the space between the nozzle's internal walls and the jet. Figure 13 shows the pitting on the orifice section due to the impact of particles as the supersonic jet impinged on the orifice lip. As the jet passes through the nozzle, flow is also entrained from the area between the walls and the jet. These flow mechanisms may be creating a vortex in the separated area that causes a pressure rise inside the nozzle. If the pressure rises above ambient, the jet leaving the nozzle is underexpanded, causing a decrease in axial thrust efficiency.

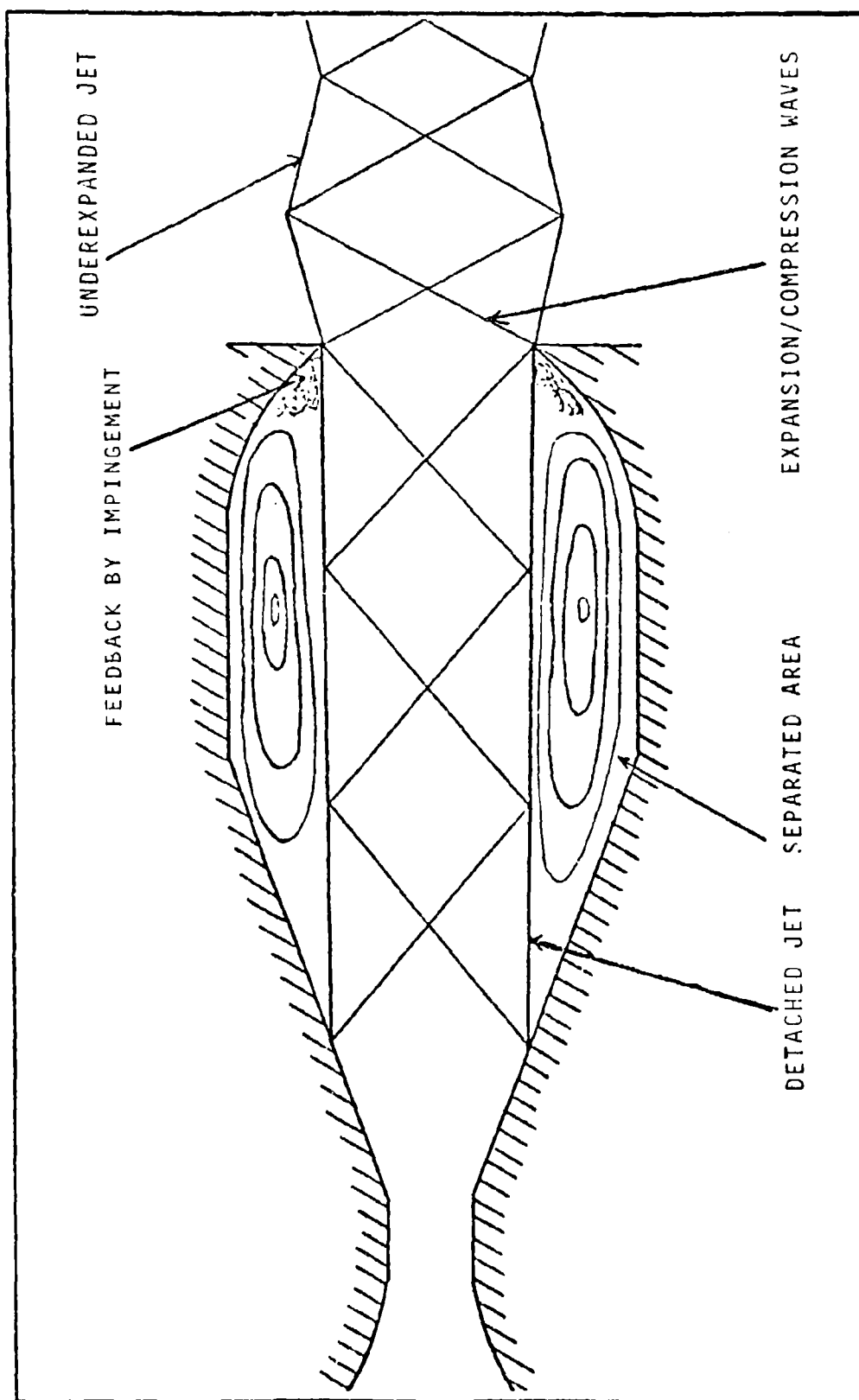


Figure 12. Undeflected Jet Operation

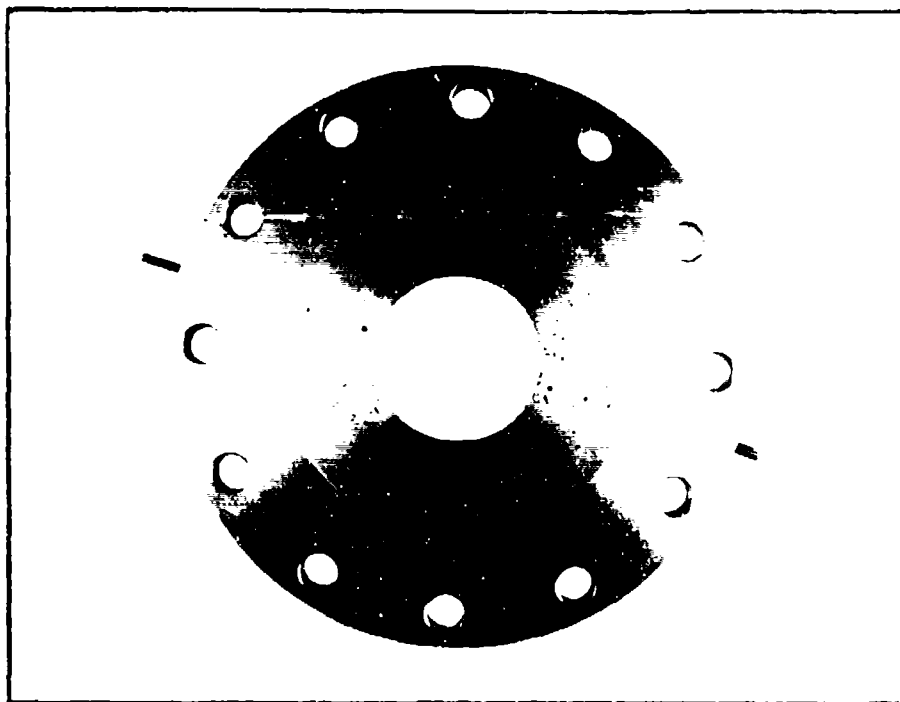


Figure 13. Orifice Section Pitting

A higher pressure in the nozzle would appear to cause the undeflected jet to be more stable since it is surrounded by a higher pressure envelope that is less effected by pressure disturbances. However, as will be explained, this is not the case.

SI Pressure Effects. Throughout all the tests conducted, one characteristic of axial thrust was prevelant. No matter what the vectoring situation was, SI pressure, number of SI ports open, or location of an active SI port, axial thrust was fairly constant at any primary supply pressure. Figure 13 shows the axial thrust that was measured over several vectoring tests.



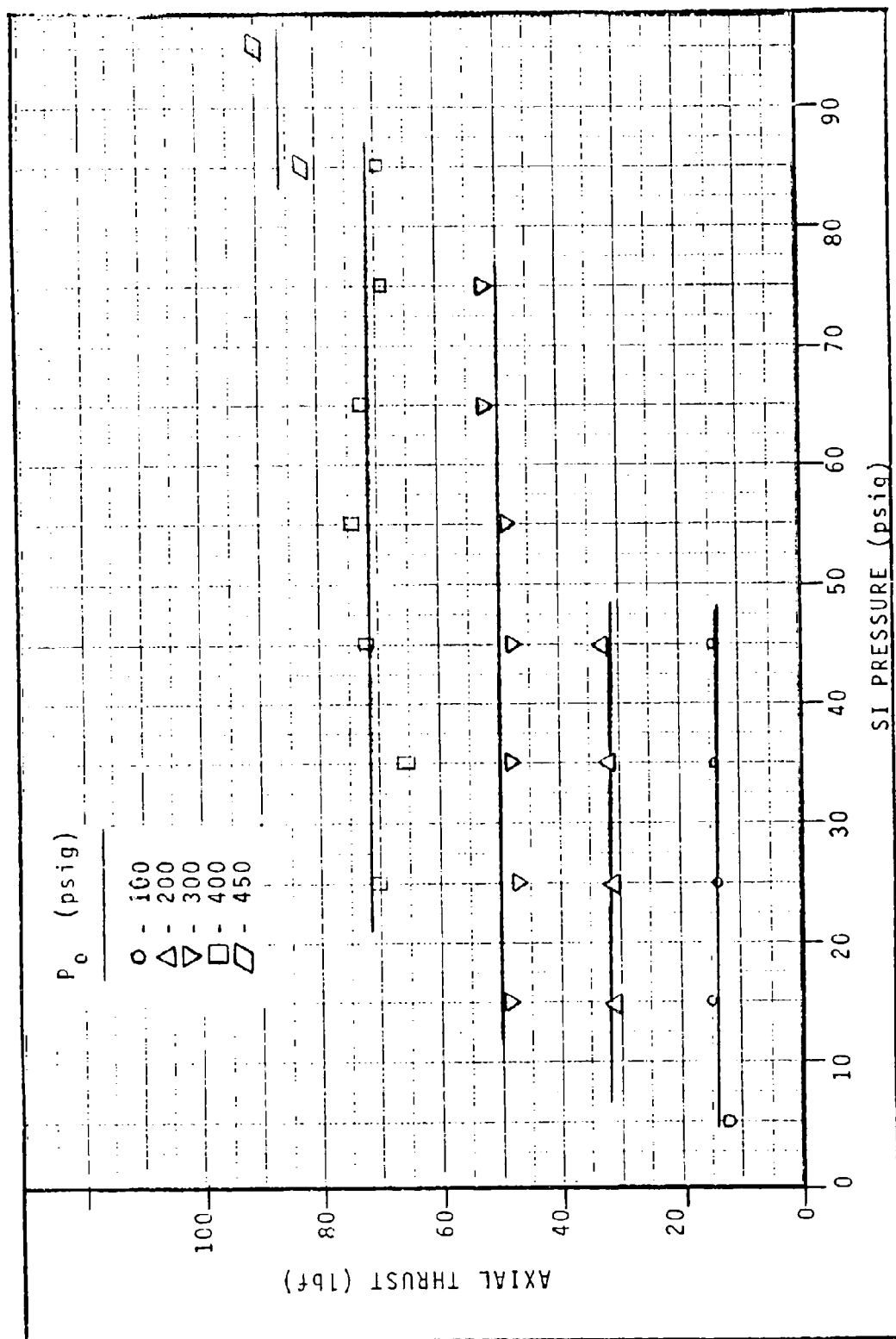


Figure 14. Axial Thrust vs. SI Pressure

### Side Force

Figure 15 shows a static pressure distribution for the nozzle when it was vectored. The primary supply pressure was 200 psig and the SI pressure was 50 psig. The pressures at the SI ports were not as low as in the undeflected case and the pressure throughout the nozzle varied. The pressure across the separated area varied in such a way that the presence of a vortex can be assumed. Near the orifice, the velocity of the vortex is toward the wall, forcing a pressure rise. In the cylindrical section, the velocity of the fluid is parallel to the wall, causing a pressure drop relative to those ports near the orifice since the pressure here is totally static. In the diverging section, the effect of the fluid turning toward the opposite wall causes a pressure increase. The jet, meanwhile, stops expanding upstream of the SI ports and adheres to the wall until it exits at the orifice. The width of the jet shown in Figure 15 is based on the effective area that would cause the static pressures measured at the wall to which the deflected jet adhered. Again, looking at Figure 13, there is a concentration of pitting on the right side of the orifice. This is the side opposite which the jet adhered and therefore, would be the side which the edge of the jet would have impinged against.

SI Pressure Effects. Figure 16 shows the side force produced for each primary supply pressure at varying SI pressures. In all cases, the SI port area is the same and only one SI port is active. This graph exhibits the three

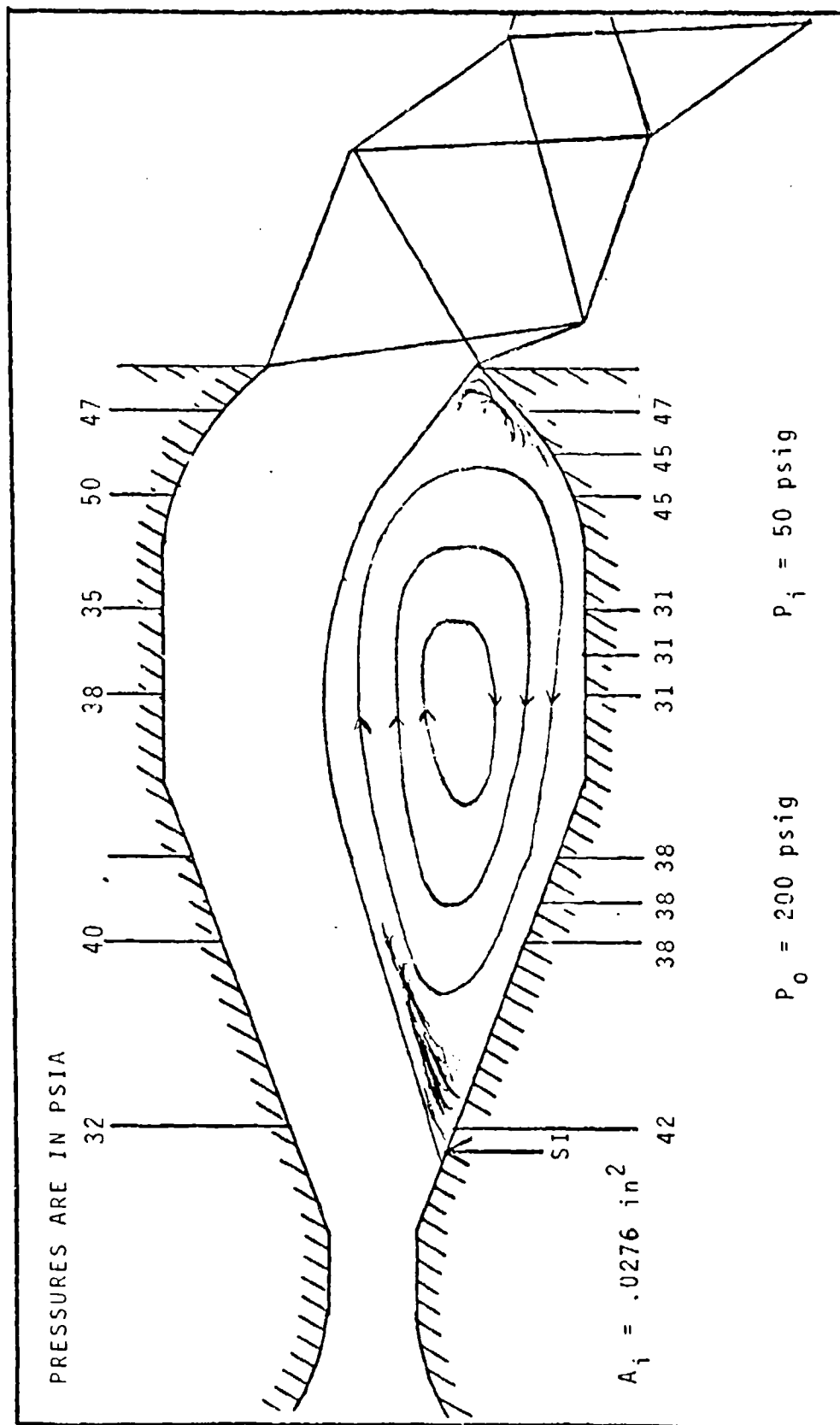


Figure 15. Vectored Configuration Pressure Distribution

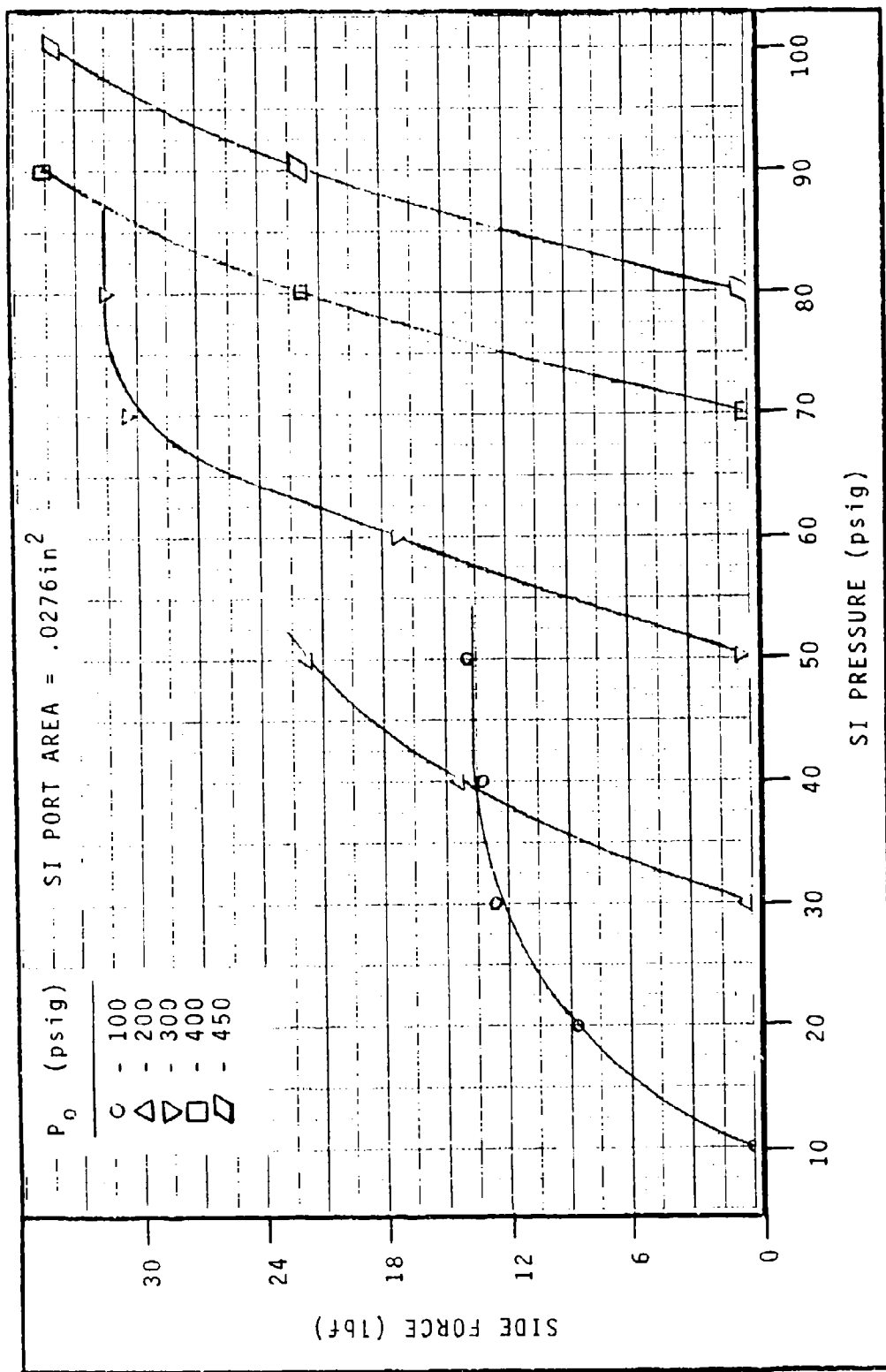


Figure 16. Side Force vs. SI Pressure

vectoring characteristics of the nozzle for a given SI port area. First, for each  $P_0$ , there is an SI pressure below which the nozzle will not produce side force. Second, the side force can be throttled over a certain range. Finally, at a  $P_0$  of 100 psig, side force begins to level off past an SI pressure of 30 psig. As will be shown later, this point was related to the choking of the SI port.

SI Port Area Effects. Similar trends in side force show up in Figure 17 which shows the amount of side force produced for a particular primary supply/SI pressure pair for varying SI port area. In all the tests, only one SI port was active. Here too, the nozzle exhibited proportional and cut-off characteristics. For each primary/SI pressure pair, there exists a minimum port diameter below which no side force is produced. However, at large port areas, the side force levels off. This too may relate to a mass flow limit as choking occurs somewhere in the SI system. However, there may be a point where the nozzle may not be able to produce anymore side force regardless of how much more mass flow a larger SI port area can support. As will be explained, none of the tests conducted could deny or confirm this.

In their work, Fitzgerald and Katz cite satisfactory vectoring at an SI port that was one-eighth of the throat diameter. In the tests conducted during this effort, data indicated that the nozzle could be vectored over a range of SI port diameters governed by supply pressure ratio ( $P_0/P_i$ ).

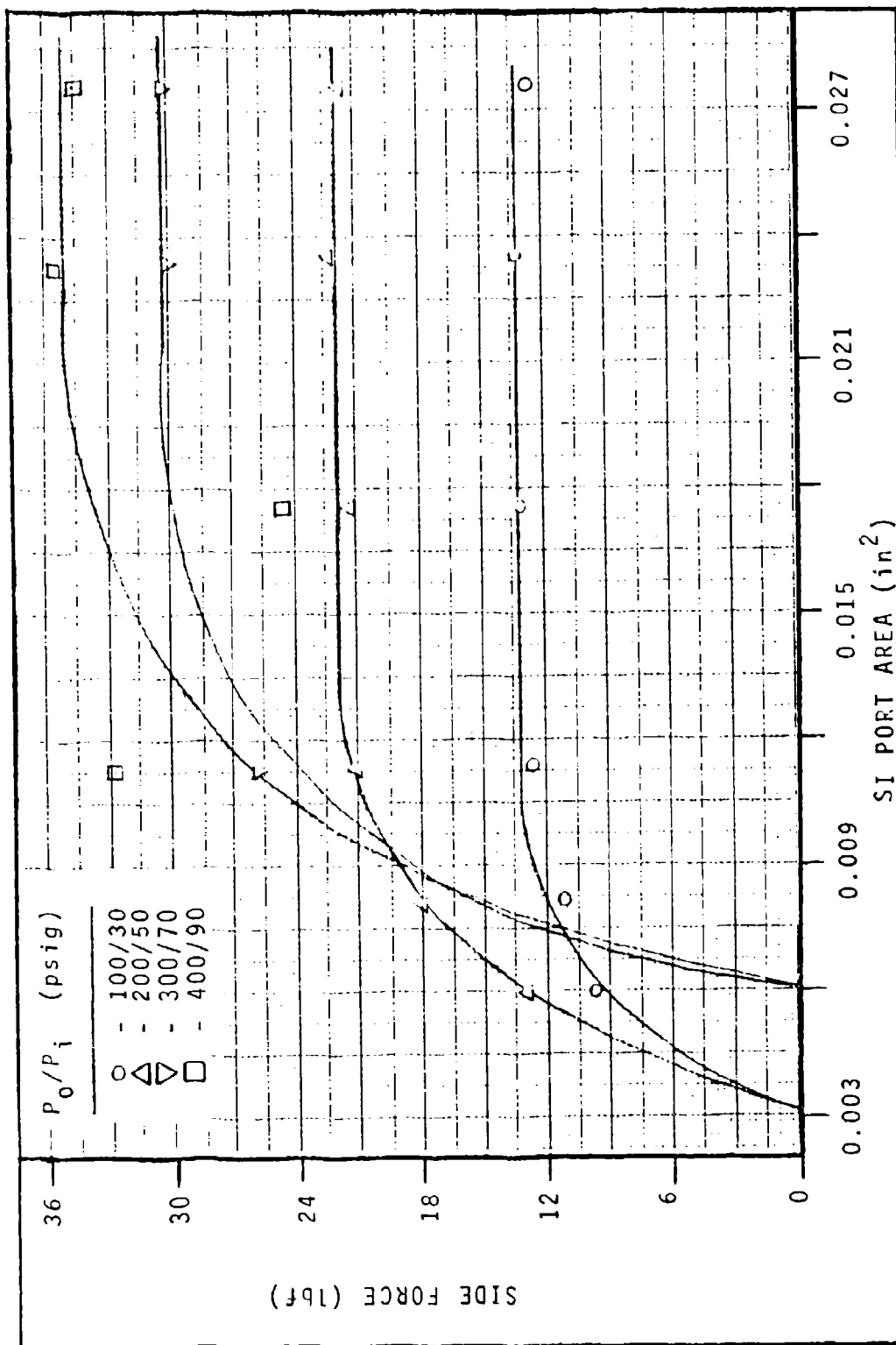


Figure 17. Side Force vs. SI Port Area

The only SI port constraint that was adhered to from the study done by Fitzgerald and Katz was the axial location of the SI ports. The ports had to be located at a given expansion ratio which was a function of the exit orifice expansion ratio. Deviation from this location, they found, caused a marked decrease in gain, efficiency, or would even yield an unvectorable nozzle.

Thrust Vector Angle. Because the nozzle had such a large maximum expansion ratio ( $A_m/A_t$ ), thrust vector angles of greater than 25 degrees were the norm. Figure 18 shows the thrust vector angle as a function of SI pressure for various primary supply pressures. The vector angle at a constant port area appeared to be a function of supply pressure ratio, except where the curve levels off at 100 psig. Since these points relate to SI port choking, the data did not indicate a vector angle limit due solely to nozzle geometry.

#### Flow Gain

The effect of altering the amount of mass flow in the SI port is a critical parameter that ties together the other stated side force trends. Mass flow gain is defined as the ratio of primary mass flow rate to SI mass flow rate. Figures 19 and 20 show side force as a function of gain. Two different sets of curves relate to tests conducted at constant SI port area with varying SI pressure (Figure 19) while the other curves are taken from the tests where SI port area was changed while supply pressure ratio was held

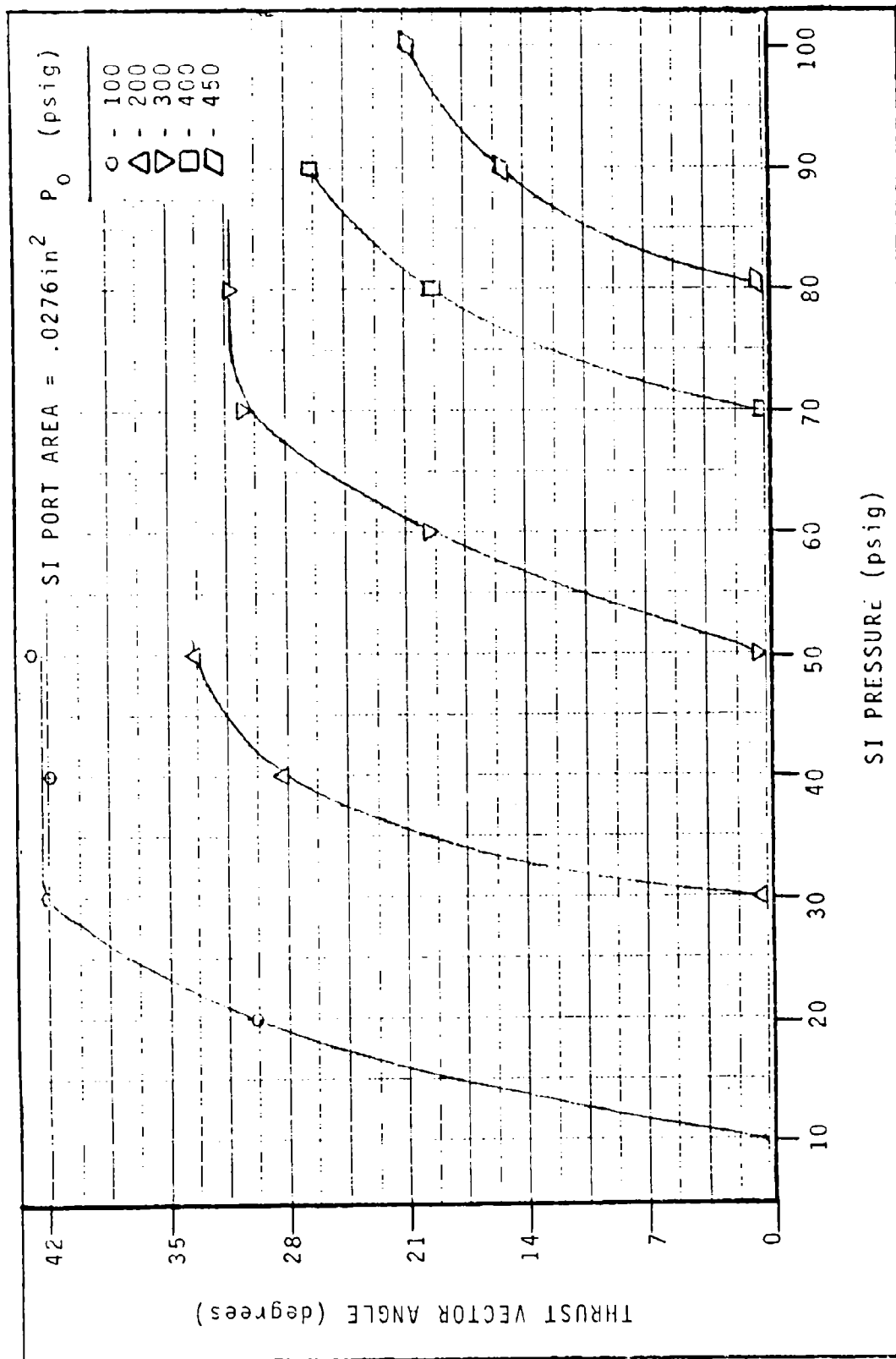


Figure 18. Thrust Vector Angle vs. SI Pressure



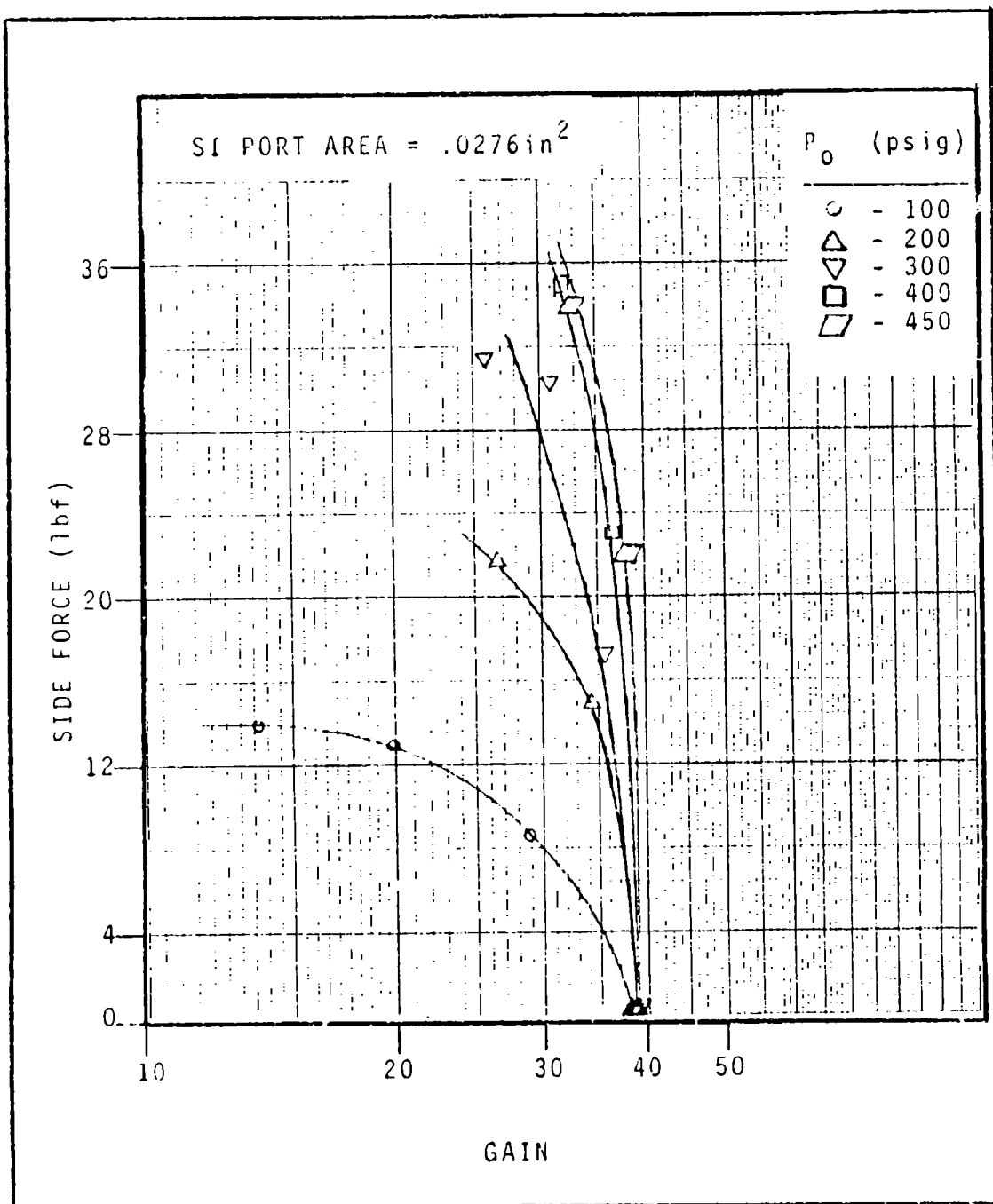


Figure 19. Side Force vs. Mass Flow Gain (Constant  $A_i$ )

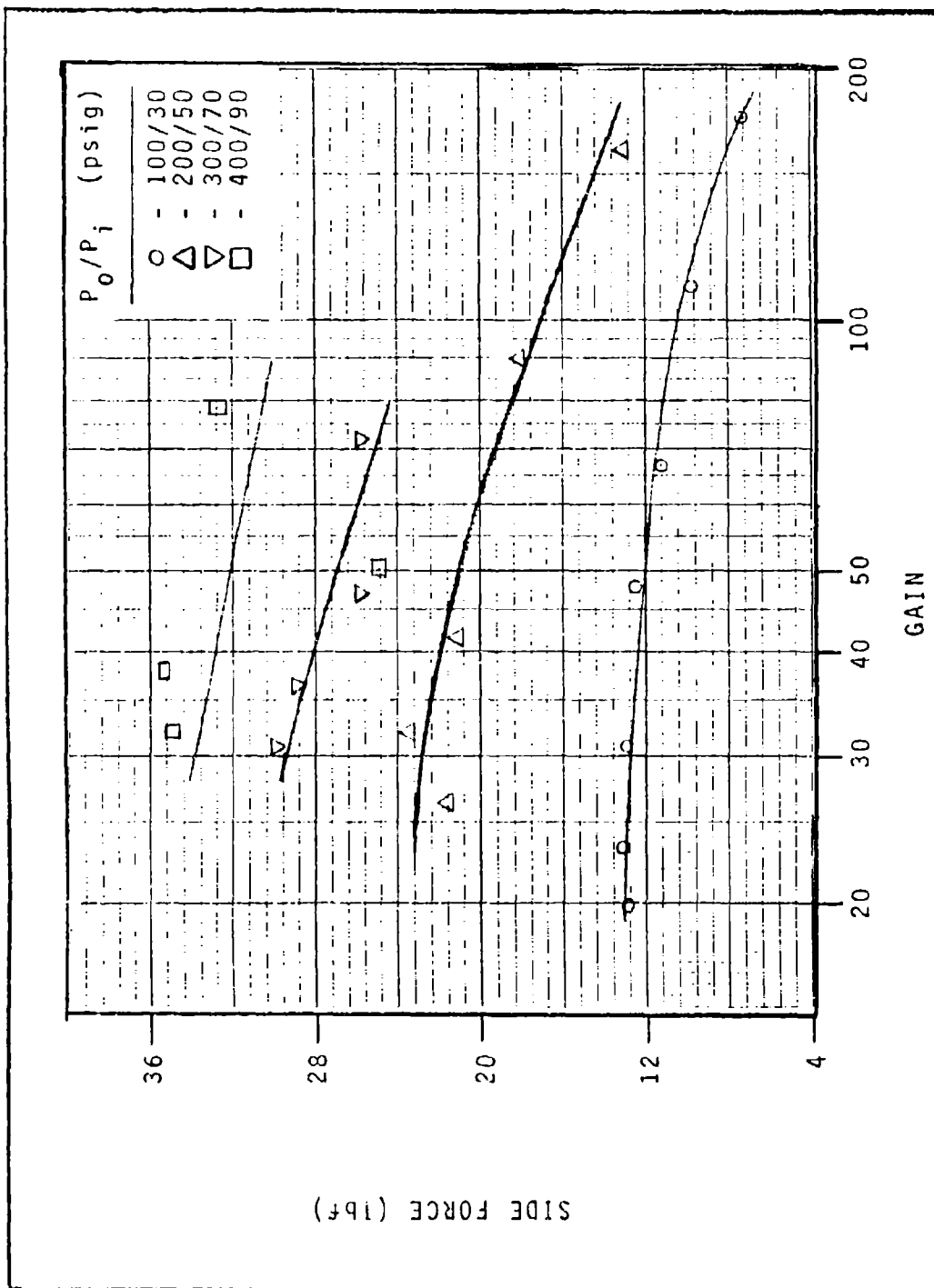


Figure 20. Side Force vs. Mass Flow Gain

constant.

It can be seen that, for a given  $P_0$ , the side force is a function of two parameters, the SI supply pressure and the SI port area. For a given SI pressure, increasing mass flow by increasing the SI port diameter increases side force (Figure 20), and for a given port area, increasing mass flow by increasing SI pressure also increases side force.

At  $P_0 = 100$  psig in Figure 19 and  $P_0 = 100/P_i = 30$  psig in Figure 20, a cut-off level appears as side force stopped increasing. For the constant area curve (Figure 19), this related to the choking of the SI port. Past 30 psig, the pressure inside the nozzle at the SI port was low enough so that the pressure ratio between the nozzle and SI supply was less than .5228, causing the flow in the SI port to be sonic and choking the flow. Although the constant SI pressure curve (Figure 20) showed the same falling off of side force increase, it is not fully clear if this was a choking of the system or if the nozzle does have an inherent limit of side force that can be produced. At the largest port diameter, an analytic study (Appendix A) of the system indicated that there were no points in the system that were near choking. However, direct mass flow measurements would be needed to confirm the system-choking assumption.

#### Nozzle Instabilities

Undelected Jet Instability. Several tests were conducted where only primary pressure was applied. Measure-

ments indicated pressure variations occurred without any parameter changes during a test. Typical results are shown in Figures 21 and 23. Schlieren video and strip chart data confirmed that during a test, the undeflected jet would start to fan out as it left the nozzle. The pressure inside the cylindrical section of the nozzle would oscillate at 4 Hz. Also, upstream near the injection ports, discrete pressure jumps would mirror each other; on one side, a pressure increase would be accompanied by a pressure drop of similar time length and pressure magnitude on the opposite wall. During a stable undeflected state, the pressure at these two points would be lower, constant, and equal. Figure 21 shows the strip chart traces of the upstream pressure transducers during an undeflected jet instability. The upstream traces were Coanda-type wall attachment (9). Downstream, the mean value of the pressure oscillation was very close to the pressure at that point at a stably vectored state. In Figures 22 and 23, the traces of the downstream transducer during a stably vectored point and an undeflected jet instability can be compared. The similarity in pressure levels, along with the upstream jet switching led to the assumption that at primary pressures of 200 psig and above, the nozzle would attempt to vector itself without any provocation. At 100 psig, the undeflected jet was completely subsonic through the orifice and no similar instability was exhibited. This instability at 200 psig and above lasted for greatly varying lengths of time but with these two

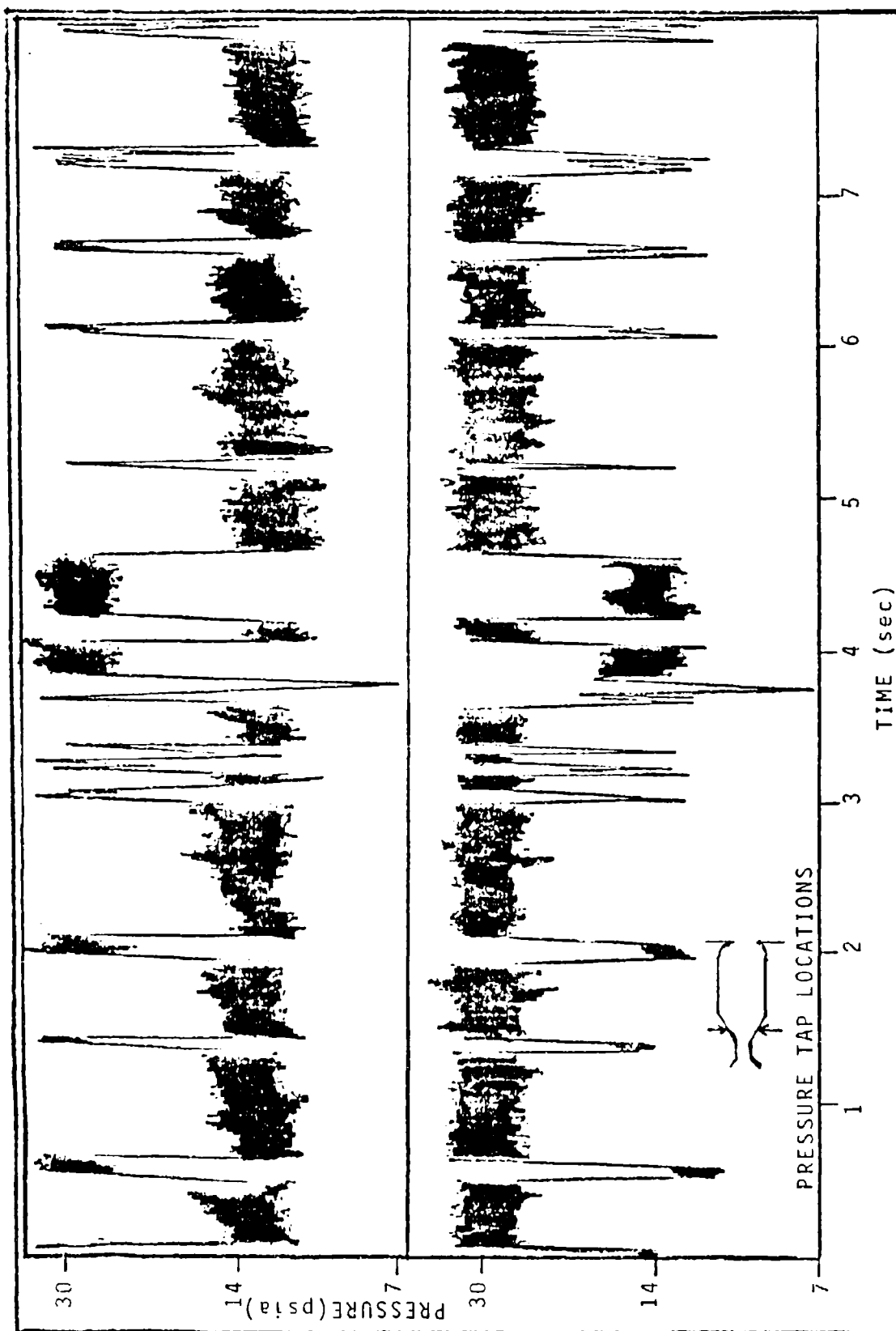


Figure 21. Upstream Transducers Strip Chart Traces During an Axial Instability

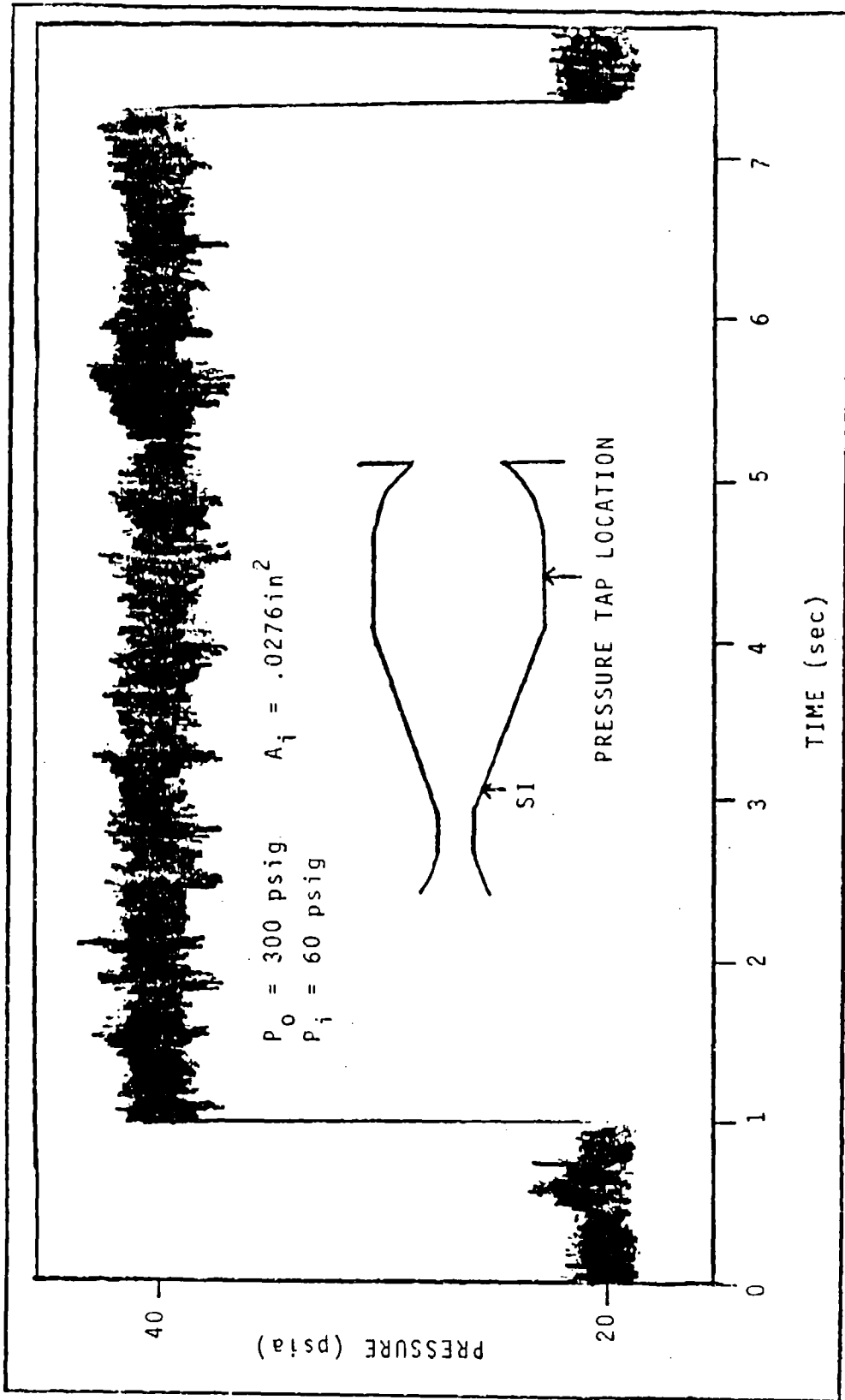


Figure 22. Downstream Transducer Strip Chart Trace During a Stable Vectoring

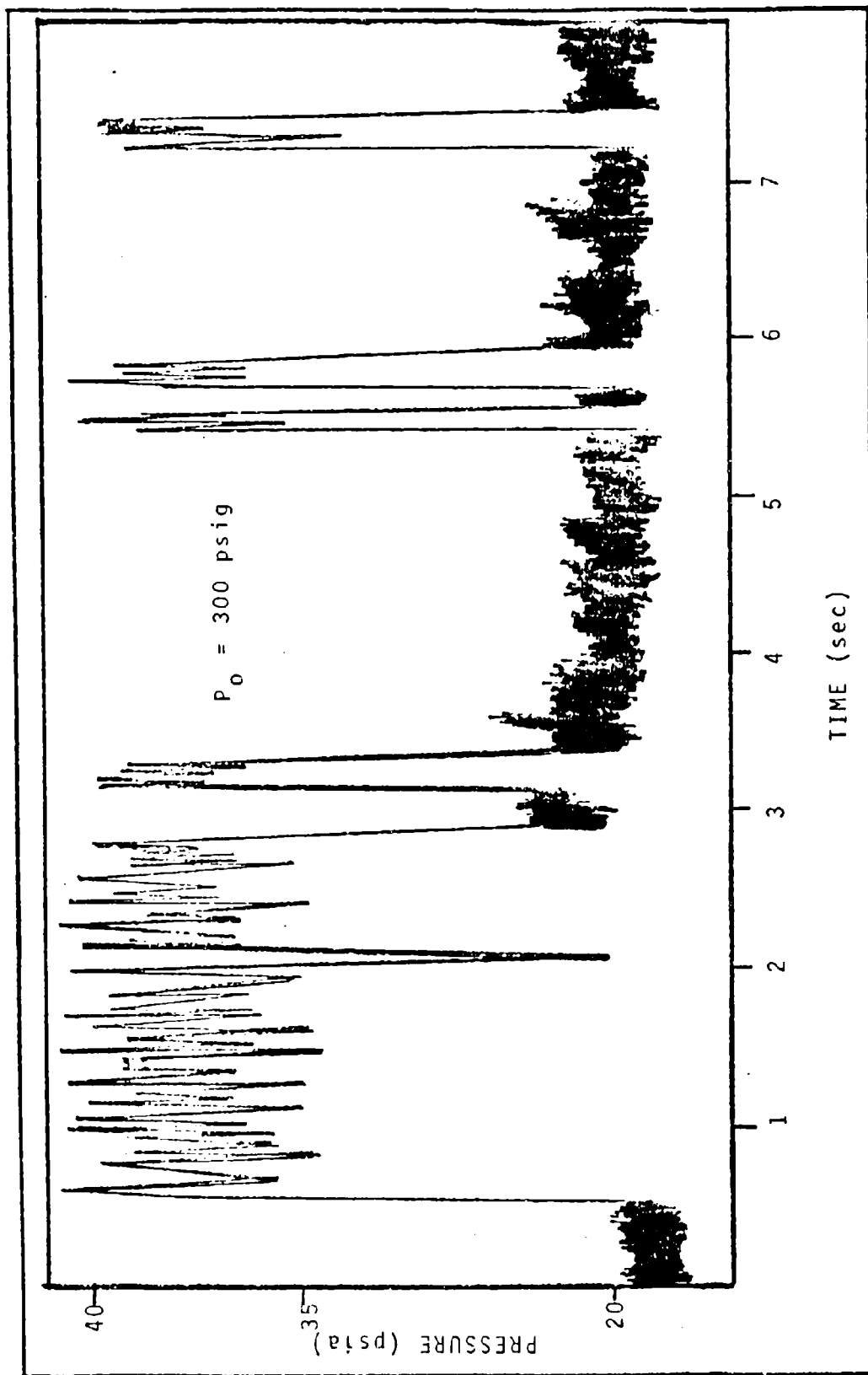


Figure 23. Downstream Transducer Strip Chart Trace During an Axial Instability

prevelant characteristics: 1) the downstream 4 Hz oscillation that was constant through a period of instability, and 2) the upstream jet attachment which would switch from side to side in an unpredictable manner and for varying lengths of time (attached to one side) during a period of instability. This type of instability was not reported by Fitzgerald and Katz (3,4).

The major differences between the nozzle tested and those studied by Fitzgerald and Katz were its longer than optimum axial spacing of the throat and exit orifice, and its large maximum expansion ratio ( $A_m/A_t$ ), 24:1. According to Fitzgerald and Katz (3:11), the only constraint on maximum expansion ratio was a lower limit of 2:1. Also, the longer axial spacing, while decreasing efficiency, should have increased stability by raising the internal pressure around the jet. These design changes point to the assumption that there may be an upper limit to the maximum expansion ratio of the nozzle. Figure 24 shows the most probable scenario for the undeflected jet instability. First, a disturbance occurs within the area of separation {1}. Next, the jet, due to the disturbance, begins to move toward the opposite wall {2}. Upstream, the jet attaches to the wall and vectoring begins {3}. Due to the fact that no mass flow is being introduced through the SI ports, there is a net decrease of mass in the separated area as fluid is entrained on the jet and leaves the nozzle. This causes a drop in pressure which, in turn, causes the jet to start



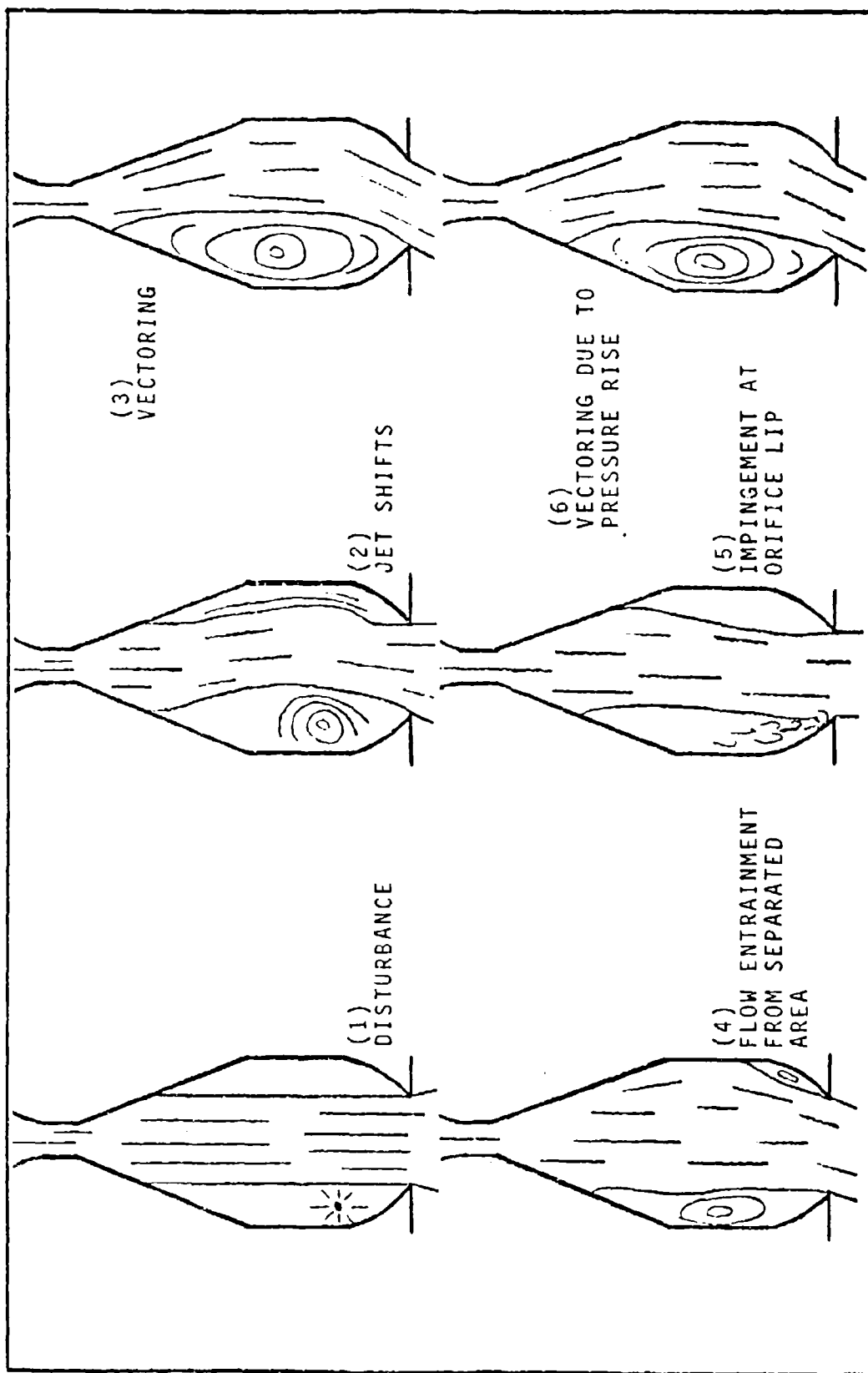


Figure 24. Undeflected Jet Instability

moving toward the axis {4} . However, there is a point where the jet begins impinging on the orifice lip to the extent that there is a net mass gain in the separated area {5} . This causes an increase in the pressure of the separated region which shifts the jet back toward the wall {6} . This process continues as a jet oscillation until an unknown mechanism causes the jet to operate stably again.

The large volume around the undeflected jet appears to be the key to why a 24:1 nozzle can be unstable while a 17:1 nozzle is not (3,4), and an even smaller nozzle will not vector (3:11). When a disturbance occurs in the area around the jet, it takes a certain amount of time for that volume of fluid to stabilize. That amount of time increases with volume. Therefore, for a given exit orifice size, the volume around the jet, and the time needed for the fluid to stabilize, increases with increasing maximum expansion ratio. However, the time needed for the jet to attach to the wall once it is disturbed is also a factor. If the pressure in the gas surrounding the jet can stabilize faster than the time it takes for the jet to attach to the wall, the axial operation will be stable. But, as it is in the case of the 24:1 nozzle used in these tests, if the jet can attach to the wall faster than the time needed for pressure stabilization, the pressure oscillations will begin. For a nozzle with a much smaller expansion ratio, the pressure could stabilize so quickly, that vectoring might not be possible even with very high pressure SI. This might ex-

plain the lower limit found by Fitzgerald and Kampe.

If varying the maximum expansion ratio of a CJTVC nozzle is not effective in controlling stable axial operation, the addition of vanes in the nozzle may stabilize the jet. In a study done at AFIT by Olson (6), vanes inserted in an axisymmetric Coanda nozzle aided the stabilization of a vectored jet by giving it a channel to which it could adhere. Although its use would not be for vectoring, the presence of crossed vanes meeting at the nozzle's axis might keep the jet in place while no SI flow is present.

Vectoring Instability at Low SI Pressure. When vectoring was attempted at lower than minimum SI pressure (as defined on the graphs presented as zero side force), a similar oscillation occurred downstream of the SI ports. However, these oscillations tended to occur at 9 Hz over all pressure ranges tested. The SI flow, either by creating more feedback at the orifice lip or by decreasing the volume of separation around the jet, was decreasing the inherent capacitance of the separated region. This caused oscillations similar to those seen with the undeflected jet, but at a much faster rate. Figures 22 and 25 show the strip chart traces of the downstream pressure tap in the cylindrical section during a stable vectoring and an unstable vectoring at low SI pressure. The 9 Hz oscillation is obvious after the ports open in the unstable configuration while the downstream pressure rose and stabilized quickly at a higher SI pressure.

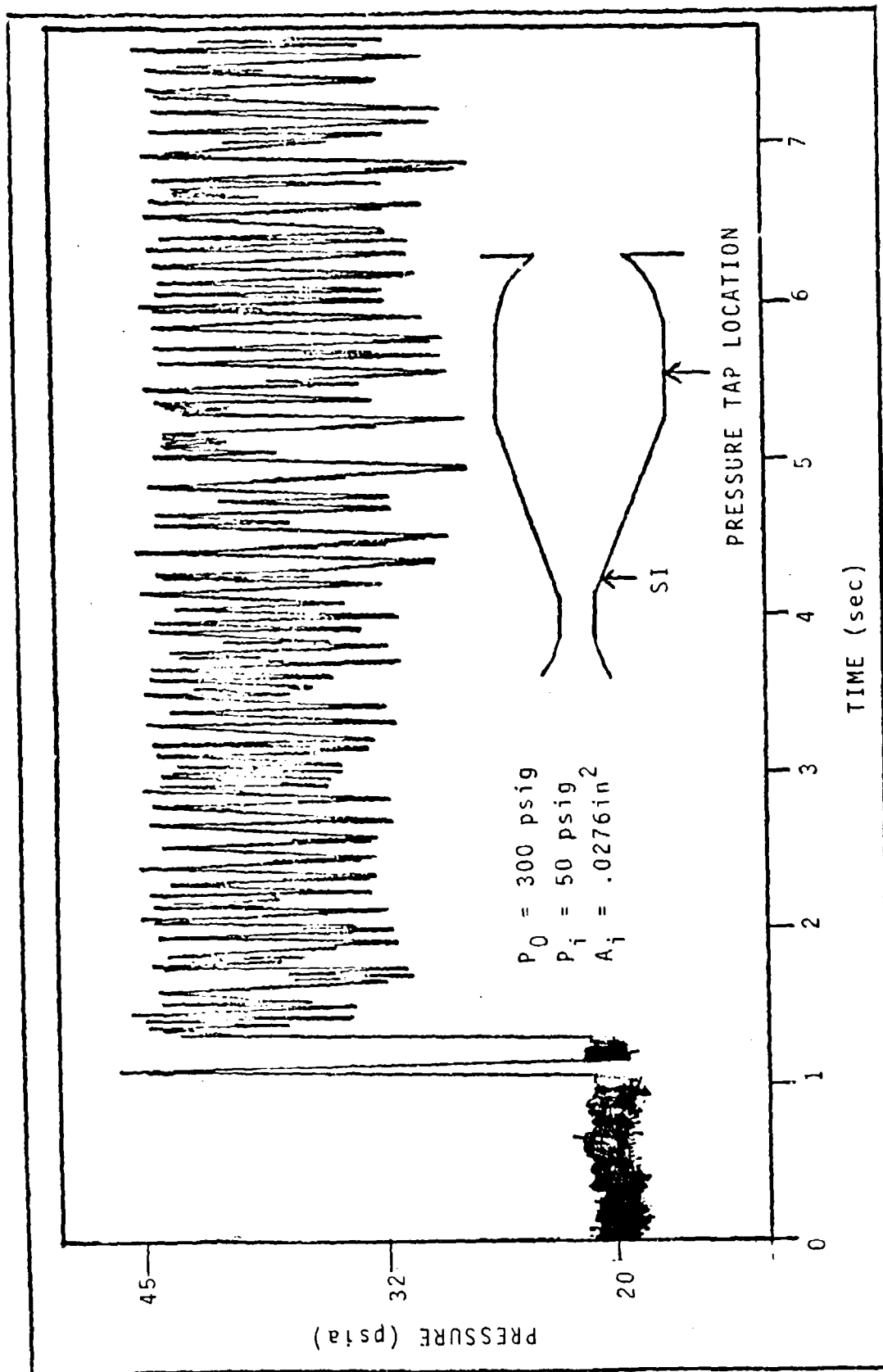


Figure 25. Downstream Transducer Strip Chart Trace During an Unstable Vectoring

Although one might conclude that stable vectoring is just a function of mass flow, the calculated flow gains do not support this. In one case, a small amount of mass flow from a high pressure source can keep the nozzle vectored while a four-fold increase in mass flow from a lower pressure supply will not. To explain why this is the case, the initial operating condition of the nozzle is to be considered.

When the nozzle is in a stable undeflected configuration, pressure at the SI ports were low enough so that injection from both a low and high pressure source could initiate a vectoring of the nozzle. But as the jet is pinched against the wall opposite the active SI port, the pressure at the SI port rises. This causes a change in SI mass flow. As the SI mass flow decreases, the jet begins to oscillate as in the unstable undeflected case. So, although the average mass flow through the SI port is relatively large, it has a cyclic pattern that causes instability. Therefore, for stable vectoring, both initial and continuous flows must be above a minimum limit, and the supply pressure must be high enough so that oscillation in the SI flow does not start after vectoring commences.

Undeflected Jet Instability With Four SI Ports Operating. An attempt was made to stabilize the undeflected jet by opening all four secondary injection ports. By introducing an injectant flow at 90 degree intervals around the jet, it was hoped that this would create either four symm-

etric areas of controlled separation or stabilize the volume surrounding the jet by raising its pressure. This was not successful. When the four ports were opened in sequence, the nozzle would vector toward the first opened port and would remain that way after the other ports were opened. Once all ports were opened, the vectoring jet would sometimes switch from one plane to another. This caused very large side force changes. Figure 26 shows the output from a test run using four open SI ports. This is compared to test output for a test using single-port vectoring. For both tests,  $P_0$ ,  $P_i$ ,  $A_i$ , and the first (or only) port opened were the same. The right-hand chart shows a large fluctuation in side force during the 10-40 second interval where all the ports were opened. Also, during the rest of the test, pulsing all SI port valves simultaneously yielded a side force that was much less than that produced when only one SI port was pulsed.

Once the jet is vectored by an input from any port, the rise in pressure inside the nozzle would tend to diminish the effect of any other input from a port whose supply pressure is the same as the initially opened port. Therefore, the jet would tend to stay vectored in the original position until some disturbance enhances another port's effect and allow the jet to move. With a high pressure source at a wall, any jet attachment would be unstable. The same situation occurred as the jet preferred one plane initially as all four ports were pulsed simultaneously. This

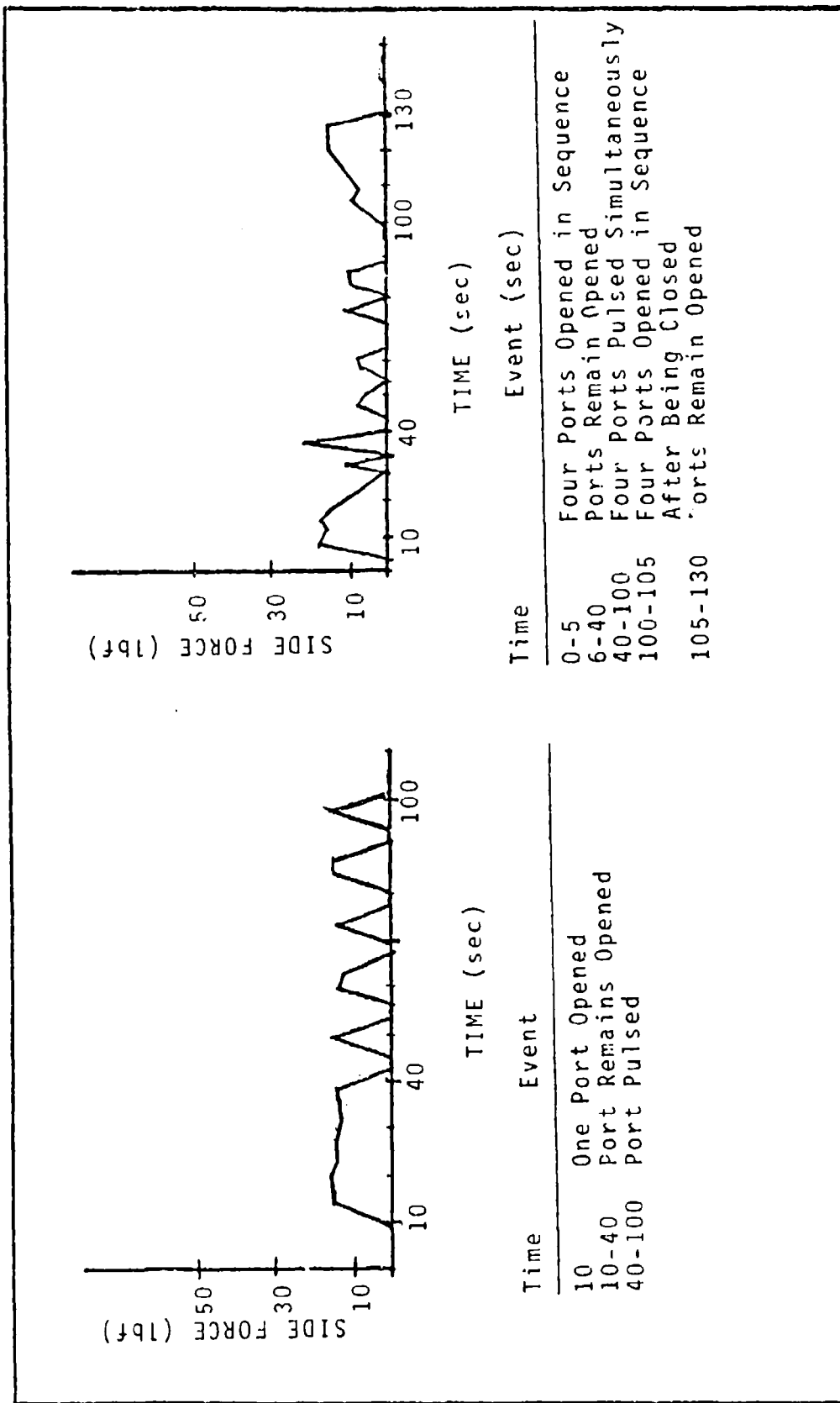


Figure 26. Test Output for Side Force vs. Time for Single-Port and Four-Port Operation

preference to one plane was most likely due to a difference in the lengths of feed lines from the manifold to the nozzle. Although the valves are opened together, there was probably varying response times for each SI port.



## V. Conclusions

For the nozzle tested, several characteristics are prevalent. The axial thrust produced by the nozzle was less than the thrust produced by conventional converging-diverging nozzles operating at the same pressure. However, regardless of the SI pressure, SI port area, or number of SI ports operating, Axial thrust was constant for a given primary supply pressure.

Side force produced is a function of SI port area and SI pressure. For a given primary supply pressure, side force increases with SI pressure until the flow in the SI port is sonic. After this occurs, the side force is constant. Side force also increases with SI port area. For a given primary supply pressure, there is an SI supply pressure below which the nozzle will not produce side force and oscillations in the nozzle will occur. There also exists, for a given supply pressure ratio, a minimum SI mass flow needed to produce side force.

Although many design criteria can be formulated from the data, one constraint should always be employed in CJTVC operation. To achieve the highest flow gain and highest side force for a given primary supply pressure, the flow in the SI port should always be sonic. This produces the highest side force and the highest gain possible with stable vectoring.

## VI. Recommendations

To continue the study of confined jet thrust vector control, the following areas should be researched:

- 1) Changing the maximum area expansion to find its effects on axial stability
- 2) Determine if there exists a limit of side force for increased mass flow at a given supply pressure ratio
- 3) Increase the operating envelope of the nozzle to confirm characteristics at higher SI and primary pressures
- 4) Construct a two dimensional CJTVC nozzle to aid in visualizing the vectoring operation and further studying undeflected jet instabilities
- 5) Investigate the effects of vanes inside the nozzle on undeflected jet instability
- 6) Utilize a scanivalve, which the control system can support, to measure a greater amount of pressure data around the nozzle
- 7) Improve flow visualization in order to prove or disprove the theories concerning axial thrust efficiency and instability.

## Appendix A: Primary System and SI System Mass Flow Calculations

Due to the absence of mass flow meters, these quantities had to be calculated from measured pressure distributions. For the primary flow, the nozzle's throat was always choked for the pressure ranges tested. The flow at the throat was assumed to be that of an ideal gas under adiabatic conditions and air mass flow was calculated using the equation:

$$\dot{m}_a = .6847 P_o A_t (g_c/R)^{1/2} T_o^{-1/2}$$

where  $\dot{m}_a$  is the primary pressure mass flow rate,  $g_c$  is a conversion constant,  $R$  is the gas constant for air, and  $T_o$  is the temperature of the primary supply (11).

For the SI flow, several factors had to be considered since the SI ports could not always be assumed to be choked. The system was modeled for analysis (Figure 27). Item 0 is the SI supply manifold. Item 1 is a solenoid valve with a 3/4" orifice. Item 2 is a flexible hose, 18" long with a 1/4" diameter. Item 3 is an SI port insert which has a varying sharp contraction at the entrance and a sharp exit into the nozzle, item 4. For the valve, a loss coefficient,  $K_m$  of .3 was chosen from typical valve data (7:354). The flexible hose was assumed to be a smooth pipe. Finally, the  $K_m$  for the sharp contraction was chosen using standard re-

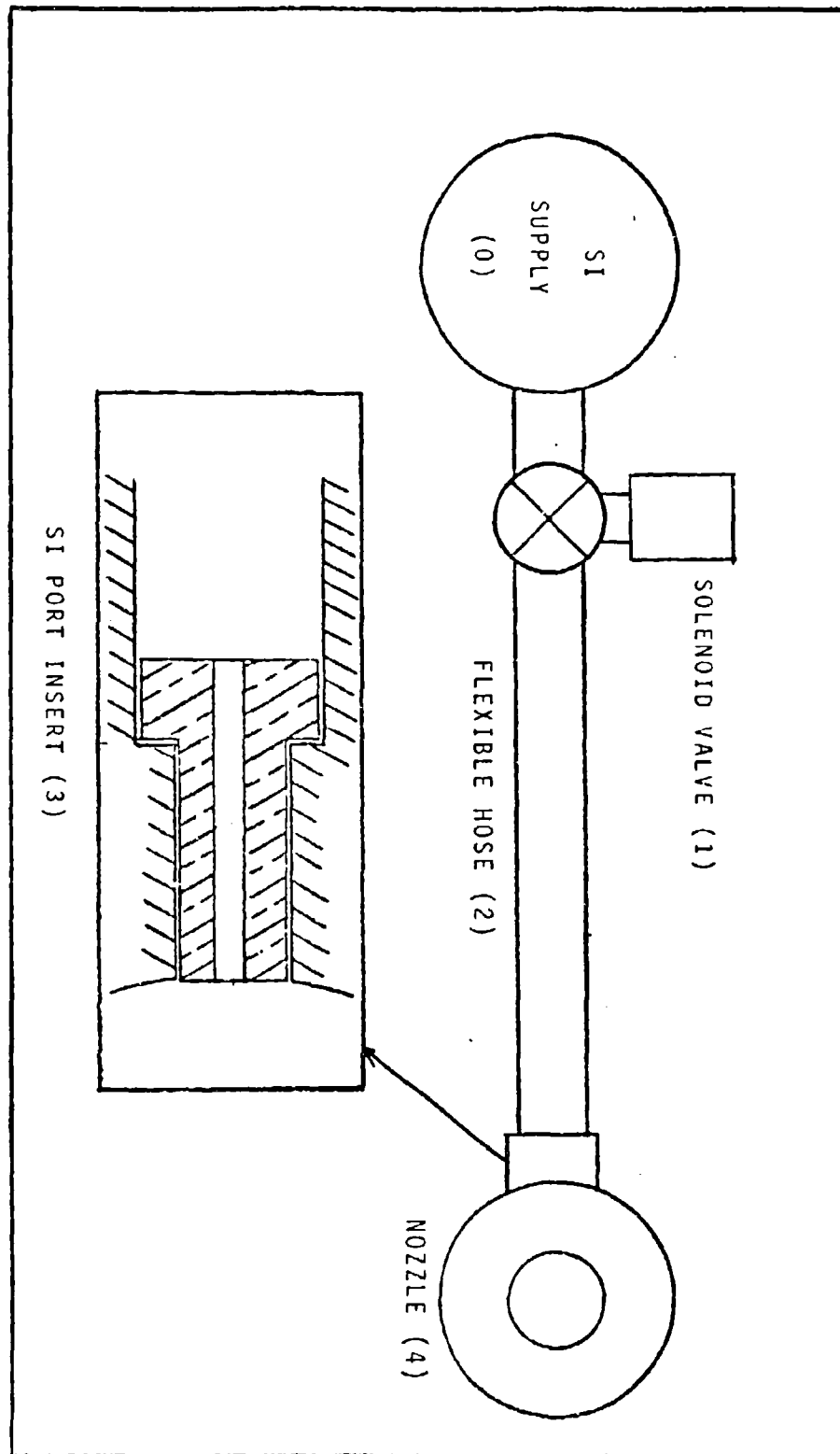


Figure 27. SI System Flow Model

lations for that geometry (7:357).

To calculate the flow rate, the velocity was assumed to be the ideal velocity based on the pressure ratio between the nozzle and SI supply manifold. This velocity was used to calculate the Reynolds number in the insert and pipe, taking into account velocity and density changes. This yielded losses for the system's components and a drop in pressure from source to nozzle:

$$\Delta P = fL\rho V^2/2D + \Sigma K_m \rho V^2/2$$

where  $\Delta P$  is the pressure drop,  $f$  is the pipe friction factor,  $L$  is the length of the pipe,  $\rho$  is the fluid density,  $V$  is the fluid velocity, and  $D$  is the pipe diameter. If the  $\Delta P$  was larger than the actual pressure drop across the system, the velocity was iterated until  $\Delta P$  was sufficiently close to the measured pressures. For the pressure ranges tested, the nominal discharge coefficient based on velocity was calculated to be .92. The nominal mass discharge coefficient,  $C_{dm}$ , was .92. Now, the mass flow gain,  $G$ , for the nozzle could be calculated:

$$G = \dot{m}_a / .92\dot{m}_i$$

where both  $\dot{m}_a$  and  $\dot{m}_i$  were the ideal mass flow based on either a choked flow (primary supply) or measured pressure ratio (SI supply).

## Appendix B: Notes on CJTVC Numerical Analysis

To analyze the operation of a vectored CJTVC nozzle (Figure 28), the main parameters to consider are the separated volume inside the nozzle,  $V_s$ , the vectored jet, and three mass flows feeding and emptying the separated volume:

$q_{si}$  - an input from the secondary injection port

$q_e$  - fluid entrained with the jet from the separated volume

$q_i$  - fluid fed back by impingement at the orifice lip

To determine the amount and effect of each flow on the separated region, the system is modeled using an electric network. The resistors in the network are related to the flow controlling mechanisms:

$R_t$  - primary flow; assumed to be choked:

$$R_t = f(A_t, T_o, C_p, M)$$

where  $C_p$  and  $M$  are the constant pressure specific heat, and the fluid's molecular weight.

$R_e$  - entrained flow from the separated region; assumed to be a function of momentum exchange:

$$R_e = f(V_j, V_s, \mu_j, \mu_s, \rho_j, \rho_s)$$

where  $V_j$  and  $V_s$  are the velocities of the jet and separated region where the two meet,  $\mu_j$  and  $\mu_s$  are the absolute viscosities of the two regions where they meet, and  $\rho_j$  and  $\rho_s$  are the densities of the two regions.

$R_i$  - feedback flow due to impingement at the orifice

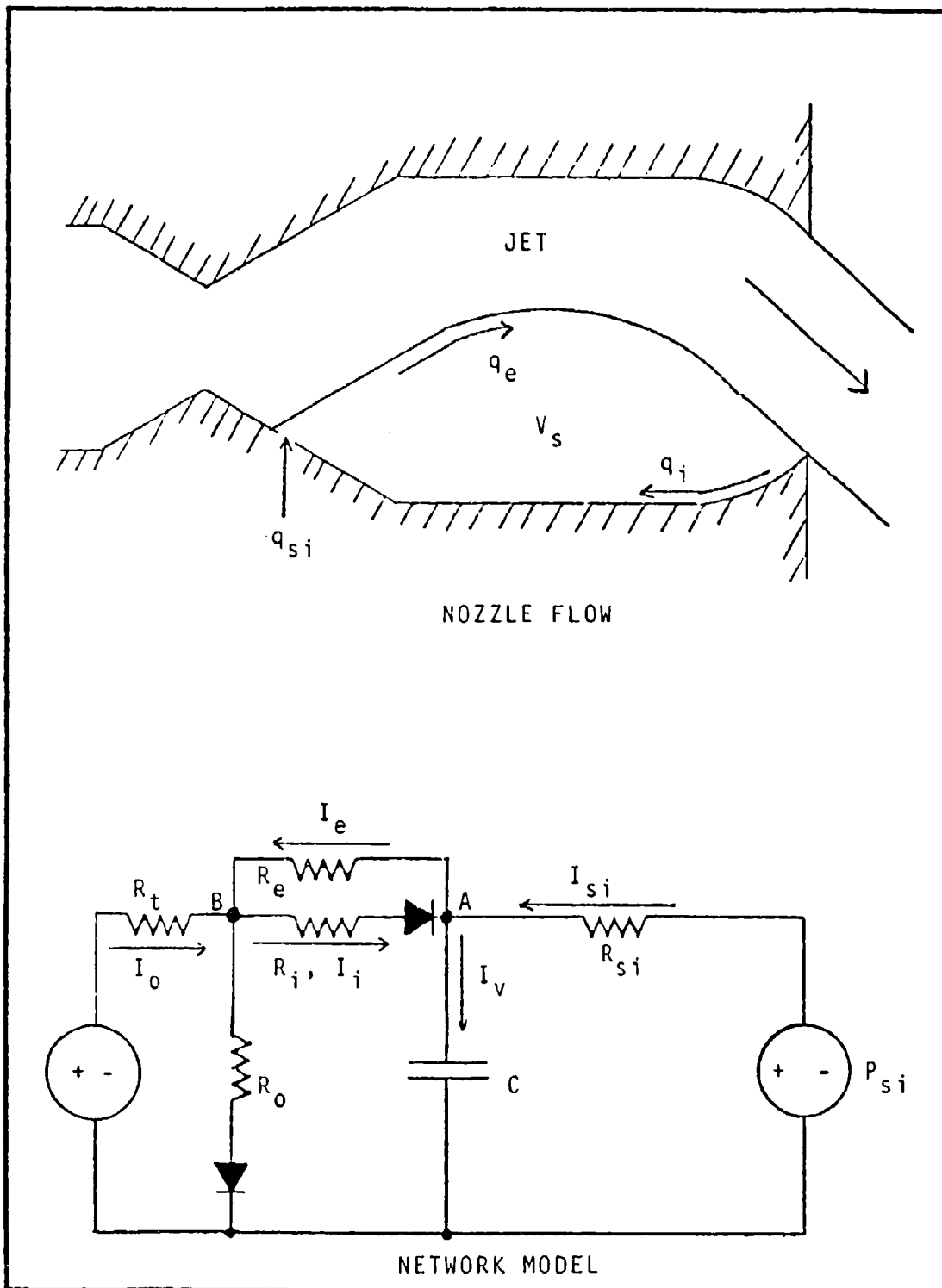


Figure 28. Vectored Nozzle Network Model

lip; assumed to be a function of geometry, flow angle, and effective jet area ratio (which can be described by jet static pressure):

$$R_i = f(A_{e0}, \alpha, P_j)$$

$R_o$  - flow out of the nozzle; assumed to be a function of flow differences only:

$$R_o = f(R_t, R_i, R_e)$$

$R_{si}$  - flow from the SI system; assumed to be sonic or subsonic:

$$R_{si} = f(P_i, P_v, f, A_i)$$

where  $P_v$  is the pressure inside the separated area.

The diodes in the network indicate assumptions made concerning flow direction in the nozzle. The two potential sources,  $P_o$  and  $P_i$ , are related to the pressure supplies. Finally, the capacitor in the system is related to the dynamics of the separated region:

$$C = dV/dP + V/\beta_m$$

where  $C$  is the capacitance of the region,  $V$  is the mean volume, and  $\beta_m$  is the fluid's bulk modulus. The compliance,  $dV/dP$ , is a function of the pressure both in the region and in the jet, and the properties of the fluid. The bulk modulus is also a function of the process by which the volume is changed:

$$\beta_m = \rho (dP/d\rho) nP$$

where  $n$  is the polytropic exponent (9).

Writing a current balance at point A:

$$I_v = I_i - I_e + I_{si}$$



where  $I_v$  is the net flow into the separated area,  $I_i$  is the flow due to impingement,  $I_e$  is the entrained flow, and  $I_{si}$  is the input from secondary injection. This balance can be rewritten:

$$C(dP_v/dt) = (P_B - P_v)/R_i - (P_v - P_B)/R_e + (P_{si} - P_v)/R_{si}$$

where  $P_B$  is the potential at point B. This potential can also be expressed in terms of other parameters:

$$P_B = P_o - I_o R_t$$

where  $I_o$  is the total flow from the primary supply.

If a solution for  $I_v$  could be found, the system's stable operating region could be calculated. Any non-constant flow would yield an unstable configuration and highly degraded side force.

For an undeflected jet, as shown in Figure 29, there would be no SI potential, and a disturbance generator,  $P_d$ , could be added. Since the components are non-linear, an impulsive disturbance could cause the system to oscillate even though  $P_o$  is a constant potential source.

These models may prove useful in a computer study of CJTVC. By modeling the flow controlling mechanisms, the operation of the nozzle could be simulated and the causes for both undeflected jet and vectoring instability might be found.

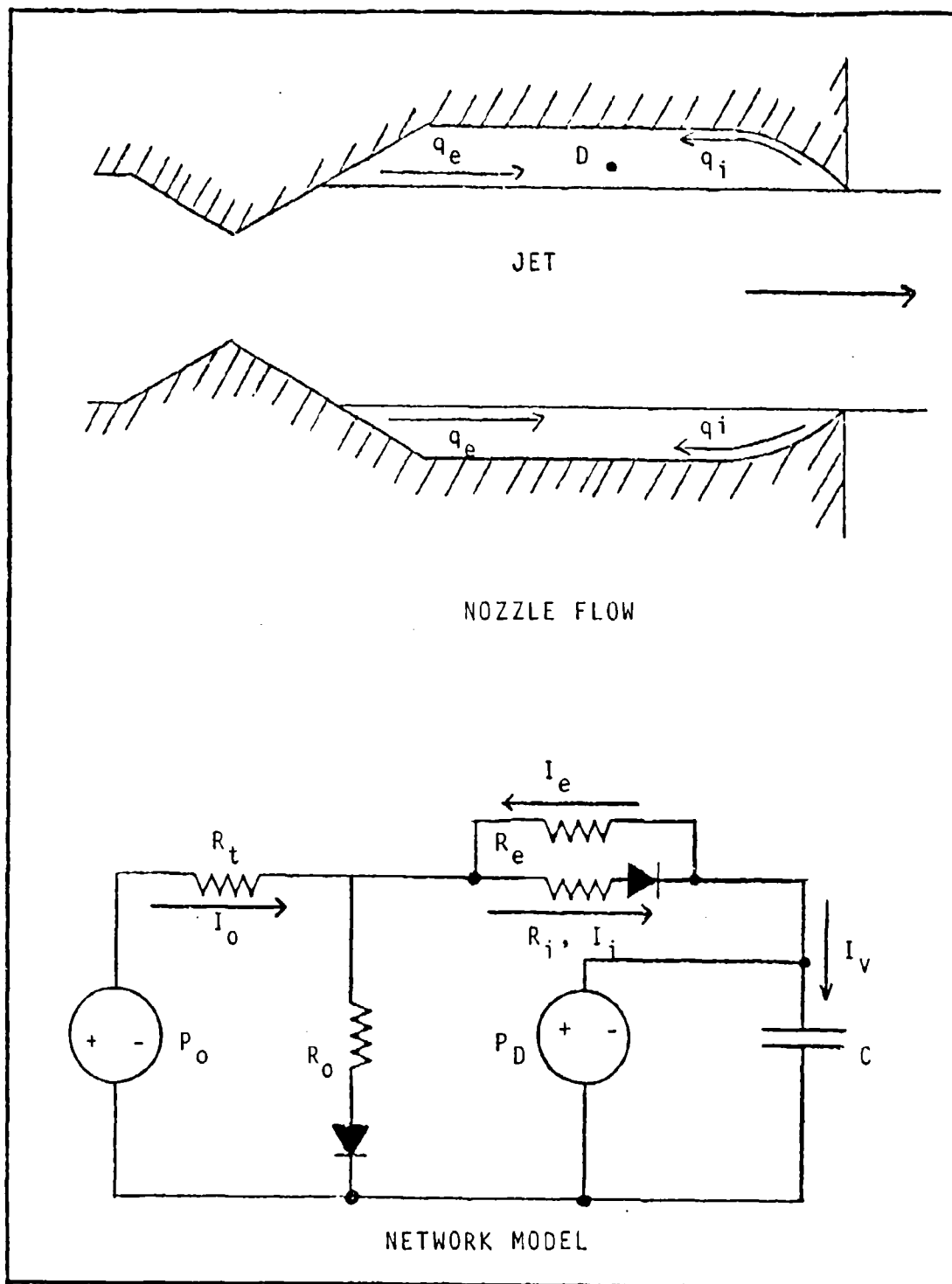


Figure 29. Axially Operating Nozzle Network Model

## Bibliography

1. Fitzgerald, R.E. and Kampe, R.F. "Boundary Layer TVC for Missile Applications," AIAA/SAE/ASME 19th Joint Propulsion Conference. AIAA-83-1153, AIAA, New York, 1983.
2. Carroll, G.R. and Cox H. "A Missile Flight Control System Using Boundary Layer Thrust Vector Control," AIAA/SAE/ASME 19th Joint Propulsion Conference. AIAA-83-1149, AIAA, New York, 1983.
3. Naval Weapons Center. Confined Jet Thrust Vector Control (CJTVC) Nozzle Development and Cold Flow Testing Program. NWC Technical Publication 6126. China Lake, CA: Technical Information Department, 1980.
4. Naval Weapons Center. Confined Jet Thrust Vector Control (CJTVC) Development and Testing Program. NWC Technical Publication 6197. China Lake, CA: Technical Information Department, 1982.
5. Shapiro, Ascher H. The Dynamics and Thermodynamics of Compressible Fluid Flow. New York: John Wiley & Sons, 1953.
6. Olson, Captain Robert E. An Experimental Investigation of a Three-Dimensional Coanda Nozzle. MS Thesis, GAM/ME/68-9. School of Engineering, Air Force Institute of Technology (AU), Wright-Patterson AFB OH, March 1968.
7. White, Frank M. Fluid Mechanics. New York: McGraw-Hill, 1979.
8. Kirshner, Joseph M. and Katz, Silas. Design Theory of Fluidic Components. New York: Academic Press, 1975.
9. Franke, Milton. Lecture notes and materials distributed in ME 5.60, Fluidics. School of Engineering, Air Force Institute of Technology (AU), Wright-Patterson AFB, OH, September 1984.
10. Chirlian, Paul M. Basic Network Theory. New York: McGraw-Hill, 1969.
11. Elrod, W.C. Lecture Notes and materials distributed in ME 7.34, Design of Air Breathing Engines. School of Engineering, Air Force Institute of Technology (AU), Wright-Patterson AFB, OH, January 1984.

## VITA

Second Lieutenant Anthony Jude Porzio was born on 15 November 1961 in Brooklyn, New York. He graduated from Stuyvesant High School in New York City in 1979 and attended Stevens Institute of Technology in Hoboken, New Jersey from which he received the Degree of Bachelor of Engineering in Mechanical Engineering with High Honors in May 1983. He received his commission through the ROTC program at Detachment 490 in Newark, New Jersey. He entered the graduate program at the Air Force Institute of Technology in June 1983.

Permanent address: 245 Windsor Place  
Brooklyn, NY 11215

UNCLASSIFIED

SECURITY CLASSIFICATION OF THIS PAGE

## REPORT DOCUMENTATION PAGE

1a. REPORT SECURITY CLASSIFICATION <b>UNCLASSIFIED</b>			1b. RESTRICTIVE MARKINGS		
2a. SECURITY CLASSIFICATION AUTHORITY			3. DISTRIBUTION/AVAILABILITY OF REPORT  Approved for public release; distribution unlimited		
2b. DECLASSIFICATION/DOWNGRADING SCHEDULE					
4. PERFORMING ORGANIZATION REPORT NUMBER(S)  AFIT/GAE/AA/84D-22			5. MONITORING ORGANIZATION REPORT NUMBER(S)		
6a. NAME OF PERFORMING ORGANIZATION  School of Engineering		6b. OFFICE SYMBOL (If applicable)  AFIT/EN	7a. NAME OF MONITORING ORGANIZATION		
6c. ADDRESS (City, State and ZIP Code)  Air Force Institute of Technology Wright-Patterson AFB, OH 45433			7b. ADDRESS (City, State and ZIP Code)		
8a. NAME OF FUNDING/SPONSORING ORGANIZATION  AFWAL/FDL		8b. OFFICE SYMBOL (If applicable)	9. PROCUREMENT INSTRUMENT IDENTIFICATION NUMBER		
8c. ADDRESS (City, State and ZIP Code)  Wright-Patterson AFB, OH 45433			10. SOURCE OF FUNDING NOS.		
11. TITLE (Include Security Classification)  See Box 19			PROGRAM ELEMENT NO.	PROJECT NO.	TASK NO.
12. PERSONAL AUTHOR(S)  Anthony J. Porzio, B.E., 2Lt, USAF			WORK UNIT NO.		
13a. TYPE OF REPORT  MS Thesis		13b. TIME COVERED  FROM _____ TO _____	14. DATE OF REPORT (Yr, Mo., Day)  1984 December		15. PAGE COUNT  69
16. SUPPLEMENTARY NOTATION					
17. COSATI CODES			18. SUBJECT TERMS (Continue on reverse if necessary and identify by block number)		
FIELD	GROUP	SUB. GR.	Propulsion, Thrust Vector Control, Secondary Injection		
21	08				
19. ABSTRACT (Continue on reverse if necessary and identify by block number)					
Title: CHARACTERISTICS OF A CONFINED JET THRUST VECTOR CONTROL <del>DEVICE</del> <b>NOZZLE</b>					
Thesis Chairman: Dr. Milton Franke					
<div>Approved for public release: 12AW AFB 100-17, 21 Feb 85 FOR E. W. WILSON Head, Research and Professional Development Air Force Institute of Technology (AFIT) Wright-Patterson AFB OH 45433</div>					
20. DISTRIBUTION/AVAILABILITY OF ABSTRACT  UNCLASSIFIED/UNLIMITED <input checked="" type="checkbox"/> SAME AS RPT. <input type="checkbox"/> DTIC USERS <input type="checkbox"/>			21. ABSTRACT SECURITY CLASSIFICATION  UNCLASSIFIED		
22a. NAME OF RESPONSIBLE INDIVIDUAL  Dr. Milton Franke			22b. TELEPHONE NUMBER (Include Area Code)  255-2362 (513)	22c. OFFICE SYMBOL  AFIT/ENY	

19 (cont.)

A study of confined jet thrust vector control (CJTVC) is presented. By isolating an area of flow separation within the body of a nozzle, CJTVC has the advantage over other thrust vector control devices using secondary injection (SI) in that it can operate independent of altitude. This makes it ideal for applications in small missiles and spacecraft attitude control. In this study, axial thrust, side force, and pressure distribution across the nozzle were measured. The parameters varied were SI pressure, primary supply pressure, and SI port area.

Results indicate that there is a lower limit to the supply pressure ratio (SI pressure to primary pressure) and SI mass flow below which, the nozzle will not produce side force. Also, above a primary pressure of 200 psig, the undeflected jet exhibits instabilities. Without SI, a 4 Hz oscillation occurs in the nozzle and switching jet attachment occurs near the throat. When an attempt is made to vector the nozzle at a below minimum SI pressure, a similar, but faster 9 Hz oscillation begins. The production of side force is limited by choking of the SI ports. Mass flow gain, the ratio of primary mass flow to SI mass flow, and side force are both found to be functions of SI port area and supply pressure ratio.